Received: 18 June 2024 | Revised: 8 January 2025 | Accepted: 29 January 2025

DOI: 10.1002/alz.70030

Alzheimer's & Dementia®
THE JOURNAL OF THE ALZHEIMER'S ASSOCIATION

RESEARCH ARTICLE

Genetic and pharmacologic enhancement of SUMO2 conjugation prevents and reverses cognitive impairment and synaptotoxicity in a preclinical model of Alzheimer's disease

Luana Fioriti[1,2] | **Nadeeja Wijesekara**[3] | **Elentina K. Argyrousi**[2] | **Shinsuke Matsuzaki**[4,5,6] | **Hironori Takamura**[3,6] | **Kanayo Satoh**[3] | **Kyung Han**[3] | **Hiroto Yamauchi**[5] | **Agnieszka Staniszewski**[2] | **Erica Acquarone**[2] | **Franca Orsini**[1] | **Annacarla Martucci**[1] | **Taiichi Katayama**[6] | **Ottavio Arancio**[2,7] | **Paul E. Fraser**[3,8]

[1]Department of Neuroscience, Istituto di Ricerche Farmacologiche Mario Negri, IRCCS, Milano, MI, Italy

[2]Department of Pathology and Cell Biology, Taub Institute for Research on Alzheimer's Disease and the Aging Brain, Columbia University, New York, New York, USA

[3]Tanz Centre for Research in Neurodegenerative Diseases, University of Toronto, Toronto, Ontario, Canada

[4]Department of Radiological Sciences, Faculty of Medical Science Technology, Morinomiya University of Medical Sciences, Suminoe Ward, Osaka, Japan

[5]MINCL, Morinomiya University of Medical Sciences, Suminoe Ward, Osaka, Japan

[6]Department of Child Development & Molecular Brain Science, United Graduate School of Child Development, Osaka University, Suita, Osaka, Japan

[7]Department of Medicine, Columbia University, New York, New York, USA

[8]Department of Medical Biophysics, University of Toronto, Toronto, Ontario, Canada

Correspondence
Ottavio Arancio, Department of Pathology and Cell Biology, Taub Institute for Research on Alzheimer's Disease and the Aging Brain, Columbia University, 630 West 168th Street, New York, NY 10032, USA.
Email: oa1@cumc.columbia.edu

Present address
Nadeeja Wijesekara, Ionis Pharmaceuticals, Carlsbad, CA, USA.

Funding information
Canadian Institutes of Health Research, Grant/Award Number: PJT-173497; Weston Brain Institute, Grant/Award Number: TR192065; National Institutes of Health, Grant/Award Numbers: NIH-NINDS R01NS110024, R01NS049442 to O.A, NIH R01NS134902 to L.F; Japanese Society for the Promotion of Science (JSPS); Fostering Joint International Research, Grant/Award Number: 17KK0197 to S.M; Grant-in-Aid for Scientific Research, Grant/Award Number: 21K06759 to

Abstract

INTRODUCTION: Amyloid beta oligomers (Aβos) are toxic to synapses and key to the progression of Alzheimer's disease (AD) and amyloid pathology, representing a target for therapeutic strategies.

METHODS: Amyloid and small ubiquitin modifier 2 (*SUMO2*) transgenics were analyzed by electrophysiology and behavioral testing. A recombinant analogue of SUMO2, SBT02, was generated and assessed for brain penetration and the ability to mitigate amyloid pathology.

RESULTS: Elevated *SUMO2* expression prevents cognitive and synaptic impairment in a mouse model of AD amyloid pathology. Systemic administration of SBT02 resulted in high brain bioavailability and prophylactically halted the progression of AD-associated deficits. SBT02 also restored cognition and synaptic function in late-stage amyloid load. Mechanistically, SUMO2 and SBT02 do not alter amyloid processing or clearance and mitigate synaptotoxicity in the presence of high amyloid loads.

DISCUSSION: SBT02 is a promising therapeutic strategy to counteract and reverse the toxic effects of Aβos in AD.

S.M; Japanese Society for the Promotion of Science; Alzheimer's Association, Grant/Award Number: AARG 17-505136 to L.F

KEYWORDS
amyloid transgenic mouse model, behavioral analyses, biologic therapy, cognition, drug development, electrophysiology, preclinical testing, small ubiquitin-like modifiers, SUMOylation

Highlights

- Genetic overexpression of human *SUMO2* prevents the long-term potentiation (LTP) impairments and cognitive deficits in amyloid precursor protein (APP) transgenics without affecting amyloid pathology.
- A recombinant analogue of human SUMO2, termed SBT02, when administered systemically, displays high brain bioavailability and has no adverse effects at high doses.
- Prophylactic treatment of APP transgenics with SBT02 prior to the development of amyloid pathology results in the prevention of synaptic and behavioral dysfunction.
- SBT02 also reverses pre-existing LTP and cognitive impairments when administered to APP transgenics with advanced and severe pathology.
- SBT02 has no impact on amyloid pathology, indicating a mechanism of action on synaptic resistance to Aβ toxicity.

1 | BACKGROUND

Therapeutic strategies against Alzheimer's disease (AD) have focused on enhancing the clearance of amyloid pathology and reducing the production and/or aggregation of amyloid beta (Aβ).[1] Symptomatic treatments have limited efficacy, and there remains a need for therapies that are capable of limiting synaptic loss and dysfunction to prevent and possibly reverse the cognitive decline in AD.[2] Small ubiquitin modifier (SUMO) proteins are an under-explored therapeutic approach, and they may fulfill this need given their roles in synaptic biology.[3]

SUMO proteins are conjugated to lysine residues of their targets, which regulates the stability, activity, folding, aggregation, and cellular location of their target proteins.[4] SUMOylation can also influence the addition of other post-translational modifications such as ubiquitination and phosphorylation and promote novel protein–protein interactions. There are three primary paralogues; SUMO1 has ≈50% sequence homology to SUMO2/SUMO3, with the latter being virtually identical as they differ by only three residues. SUMOylation is activated by the sentrin/SUMO-specific proteases (SENPs), which cleave C-termini residues to expose a di-glycine motif necessary for conjugation.[5] Immediately following the SENP proteolysis, SUMO proteins are activated by the ATP-dependent E1 enzymes (SUMO-activating enzyme subunit 1/2 [SAE1/2]), and subsequently transferred to Ubc9 (ubiquitin conjugating enzyme 9), which unlike ubiquitination is the only E2 ligase in this enzymatic cascade. Conjugation is facilitated by a collection of E3 ligases that have been identified and confer the required specificity for individual target proteins.[4] As with the activation, de-conjugation is mediated by the same SENP group of proteases.

SUMO post-translational modifications play a number of pivotal roles in synaptic function and synaptic plasticity.[3,6] Super-resolution microscopy using multiple antibodies has demonstrated the co-localization of SUMO2 with the presynaptic synaptophysin and post-synaptic marker PSD 95 (postsynaptic density protein 95).[7] This is consistent with the presence of the enzymatic machinery required for SUMOylation in synaptic compartments. This has several functional consequences, such as the direct modification by SUMO1 of active zone protein Rab3-interacting molecule 1α (RIM1α) and its regulation of synaptic vesicle exocytosis.[8] Neurotransmitter release is also enhanced by blocking SUMO1 modification of syntaxin 1A and modulating its interaction with the SNARE (soluble-N-ethylmaleimide-sensitive factor attachment protein receptor) complex.[9] In addition, activation of metabotropic glutamate receptor 5 (mGluR5) results in the retention of Ubc9 within synapses, leading to increases in protein SUMOylation.[10] This has functional consequences for the SUMO modification of the fragile X mental retardation protein (FMRP) and its control of dendritic spine maturation and elimination.[11] SUMO2 conjugation has also been implicated in local protein synthesis at synapses following glutamatergic stimulation.[12,13]

SUMOylation has been linked to AD and related neurodegenerative disorders, including Huntington's and Parkinson's diseases, and two of the major paralogues, *SUMO1* and *SUMO2*, exhibit disparate effects on pathogenesis and disease progression, likely due to isoform functional heterogeneity.[14–17] SUMOylation is also involved in stress granule assembly and disassembly, which is associated with Chromosome 9 open reading frame 72 (C9ORF72) neurodegeneration in amyotrophic lateral sclerosis (ALS).[18,19] Under basal conditions, SUMO1 is largely conjugated to target proteins and exacerbates amyloid pathology, tau phosphorylation, and aggregation, and *SUMO1*

overexpression leads to a reduction in dendritic spine densities.[14,20,21] In contrast, SUMO2 conjugation is essential for long-term potentiation (LTP), a type of synaptic plasticity thought to underlie memory formation and hippocampal-dependent learning,[22] and provokes a neuroprotective response to stress such as transient ischemia.[23] Moreover, SUMO2/3 conjugation is reduced both in the Tg2576 mouse model of amyloid deposition and in patients with AD.[22] Therefore, we tested the hypothesis that an increase in SUMO2/3 conjugation may represent a potential therapeutic avenue to counteract Aβ-induced synaptotoxicity as well as learning and memory deficits in AD.

RESEARCH IN CONTEXT

1. **Systematic review**: The causative link between amyloid and Alzheimer's disease (AD) has led to the development of therapeutic strategies and clinical trials. The small ubiquitin-like modifier (SUMO) family of proteins plays key roles in synaptic biology and is associated with neurodegenerative diseases.
2. **Interpretation**: Our investigation has revealed that genetic overexpression of human *SUMO2* prevents the synaptic damage that typically manifests as the clinical features of AD. This can be replicated by a recombinant analogue of SUMO2, called SBT02, which when administered subcutaneously, is brain penetrant. SBT02 was shown to prevent and also reverse synaptic dysfunction in the presence of AD-related amyloid pathology.
3. **Future directions**: Future studies will expand on this preclinical testing to determine the optimal SBT02 dose and comprehensive toxicology assessments. This will allow for the advancement of the SBT02 biologic therapy to clinical trials for AD and related disorders.

2 | METHODS

2.1 | SUMO2 and APP transgenic mouse models

All mouse work was approved by the Institutional Animal Care and Use Committee (IACUC) of the University of Toronto and the University Health Network in accordance with the regulations of the Canadian Council on Animal Care and the IACUC committee of Columbia University. The amyloid precursor protein (APP) (TgCRND8 [CRND is the acronym of the Research center wehre the animals were generated: Centre for Research in Neurodegenerative Diseases]) transgenic mice expressed full-length APP695 containing the Indiana and Swedish mutations within the Aβ sequence also using the prion costet promoter.[24] Transgenics expressing the full-length human *SUMO2* were also generated with the prion cost-tet promoter such that the *SUMO2* and *APP* transgenes were expressed in comparable cell types. Our laboratory generated the *SUMO2* overexpressing transgenics on an FVB background and, when crossed with APP mice, were maintained on a mixed 129S1/FVB background. Correspondingly, APP (129S1) were crossed to non-transgenic (Non-Tg) FVB mice to generate control mice on an identical background for the purpose of these investigations. Non-Tg animals are the littermates of TgCRND8 mice (APP ±). SUMO2+/+ APP ± double transgenic (SUMO2-APP) mice were produced from crosses of SUMO2+/+ transgenics with APP ± animals. Both male and female mice were examined at the 9-month endpoint under investigation.

2.2 | Immunoblotting and antibodies

Samples (5–45 µg total protein) were run on 4%–12% Novex tris-glycine gels (Life Technologies), and immunoblotting was performed as described previously.[20] The antibodies used were: Rabbit polyclonal SUMO2 (1:1000), which was generated and affinity-purified using methods described previously[21]; rabbit monoclonal SUMO1 (1:1000; C21A7, Cell Signaling Technology); rat monoclonal SUMO2/3 (1:1000; 3H12, Millipore Sigma); rabbit polyclonal Ubc9 (1:1000; Abcam, ab33044); rabbit polyclonal PSD-95 (1:1000; Abcam, ab18258); rabbit monoclonal Homer1 (1:10,000; Abcam, ab184955); mouse monoclonal synaptophysin (1:20,000; Abcam, ab32127); mouse monoclonal Actin (1:10,000; AC-74, Millipore Sigma); and rabbit monoclonal GAPDH (1:10,000; 14C10, Cell Signaling). Full-length APP and C-terminal fragment of APP levels of cell lysate and brain lysate were analyzed by immunoblotting using the monoclonal antibody C1/6.1.[25] After washing, horseradish peroxidase (HRP)–conjugated anti-mouse (1:3000), anti-rabbit (1:5000), anti-rat (1:5000), or anti-goat (1:5000) was applied for 1 h at room temperature (RT), and bands were visualized by enhanced chemiluminescence (ECL). Multiple immunoblots were analyzed for the quantification of PSD-95 levels and individual blots were normalized to glycerate 3-phosphate dehydrogenase (GAPDH) levels, followed by standardization based on the saline control, as described previously.[26] Quantification of all immunoblots was performed on an Odyssey Imaging System (Li-Cor Biosciences) as per the manufacturer's protocols.

2.3 | ELISA quantification of soluble/ insoluble Aβ42 and APP processing

Prior to tissue collection, all animals were perfused extensively with phosphate-buffered saline (PBS) through cardiac puncture. Vascular clearance was confirmed by the absence of any vessel staining in immunohistochemistry with anti-mouse antibodies, and quantification of SBT02 for pharmacokinetics would be due to brain uptake and not vascular contamination. Frozen brain hemispheres or dissected brain regions (cortex, hippocampus, and cerebellum [Cb]) were weighed for whole protein extraction. Tissues (100 mg) were homogenized in 500 µL of buffer containing 20 mM Tris, pH 7.4; 0.25 M sucrose; 1 mM ethylenediaminetetraacetic acid (EDTA); 1 mM EGTA and EDTA-free protease inhibitors (Millipore Sigma); and 50 mM N-ethylmaleimide (NEM) to inhibit deSUMOylation followed by son-

ication. Homogenates were centrifuged for 5 min at 27,000 × *g* and supernatants were collected. Protein quantification was performed by Bradford assay (BioRad) using the microplate format, as per the manufacturer's instructions. Readings were performed on a Spectra Max i3 (Molecular Devices). Samples were diluted in homogenization buffer to a 3 or 6 mg/mL concentration and stored in an equal volume of Laemmli buffer at −80°C. Using the hippocampal, cortical, and cerebellar lysates described, both soluble and insoluble forms of Aβ40/42 were measured using commercially available enzyme-linked immunosorbent assay (ELISA) kits (IBL International) as described previously.[27] Soluble Aβ40/42 is extracted from a 10% (w/v) tissue homogenate (20 mM Tris-HCl; 0.25 M sucrose; 1 mM EDTA/EGTA) using an equal volume of 4% diethylamine in 100 mM NaCl. The insoluble amyloid is obtained by centrifugation (100,000 × *g* for 1 h) and extracted by sonication using cold formic acid. Quantification of the endogenous murine Aβ40/42 was performed by ELISA (Invitrogen).[20] Levels of the secreted APP β-fragment (sAPPβ/Sw) in the APP-Tg and SUMO2-APP transgenics were assessed using the commercially available ELISA (IBL), which was used following the manufacturer's protocol.

2.4 | Isolation of synaptosomal fractions

Synaptosomes were prepared using an established protocol described by Von Mollard and colleagues.[28] Briefly, perfused and dissected cortical tissue was homogenized in 10 volumes of sucrose. Cellular debris was removed by centrifugation at 3000 × *g* (2 min), and the synaptosome-containing fraction was isolated by centrifugation at 14,000 × *g* (12 min), which was suspended in 320 mM sucrose and loaded onto a discontinuous 13%–5% Ficoll 400 gradient in buffer containing 320 mM sucrose and 5 mM HEPES at pH 7.4, and centrifuged in a Beckman SW41 rotor for 35 min at 22,500 rpm. Synaptosomes in the 9% layer were collected and diluted in buffer containing 140 mM NaCl, 5 mM KCl, 20 mM sodium HEPES, (pH 7.4), 5 mM $NaHCO_3$, 1.5 mM Na_2HPO_4, 1 mM $MgCl_2$, 10 mM glucose, and a purified synaptosome fraction was pelleted by centrifugation at 14,000 × *g* for 15 min.

2.5 | Immunohistochemistry and image analysis of amyloid loads

Brain hemispheres were fixed in 10% formalin (Millipore Sigma) overnight at 4°C and then immersed in 70% ethanol. Serial sections (5 µm) of paraffin-embedded tissue were stained for amyloid plaques. Amyloid deposits were identified using an HRP-conjugated primary Aβ-specific antibody (6E10-HRP, Signet) and visualized with 3,3′-diaminobenzidine (DAB) following pre-treatment with 70% formic acid. Dense and diffuse plaque staining was assessed by measuring the amyloid positive area over the total area.[20] Briefly, immunostained sections (5 µm) were scanned with Mirax Scan (Zeiss) and assessed using ImageScope (Aperio). Slides were scanned using the Mirax Scan v. 1.11 software and Zeiss Mirax Slide Scanner at 20X magnification with a Zeiss 20X/0.8 objective lens and a Marlin F146-C CCD camera. The rendered digital images were analyzed using the color deconvolution algorithm in the Aperio Imagescope software, as described previously.[29] Red, green, and blue (RGB) values were determined for both the applied hematoxylin and DAB stains. DAB was chosen as the positive color channel for identifying and quantifying Aβ-stained plaques within different areas of the brain (cortex and hippocampus). Recognition and measurement of dense and diffuse plaque areas were achieved by setting the threshold values of color intensity. The strong positive threshold was set to 80, correlating with dense staining. The medium positive threshold was set to 160, correlating with medium/diffuse staining, and the weak positive threshold was set to 0. In this way, the amyloid-positive area, as well as the intensity of Aβ staining, was quantified in different brain regions, allowing for the quick, objective comparison between brains from different animals.

2.6 | SBT02 and SBT07 expression and purification

The human SUMO2 construct was inserted into the pET-28 expression plasmid using XbaI and BamHI restriction sites. SBT02 consists of the full-length SUMO2 with hexa-His tag and leader sequence (HHHHHH-PMSDYDIPTTENLYFQGA) with a tobacco etch virus (TEV) cleavage site (GA) and hexa-His tag immediately N-terminal to the SUMO2 sequence. The inactive SBT07 contained a mutated C-terminal conjugation site where the di-glycine (GGVY) was substituted with alanine residues (AAVY). Proteins were expressed in *Escherichia coli* grown in Terrific Broth containing antibiotic (50 µg/mL kanamycin) with induction (1 mM IPTG) at 37°C for 4 h. Cell pellets were resuspended in buffer (20 mM HEPES, 300 mM NaCl, 20 mM imidazole; pH 7.4) and lysed by sonication. Lysates were clarified by centrifugation (10,000 × *g*) and applied to a nickel affinity column (Qiagen Superflow). Bound protein was washed with buffer containing 40 mM imidazole and eluted with 300 mM imidazole. Eluates were pooled and buffer exchanged by dialysis to PBS with 1 mM dithiothreitol. Protein was concentrated using Amicon Ultra-15 with a molecular weight cutoff of 10 kDa and purified by size exclusion column (Cytvia Superdex 75) in PBS. Fractions containing purified SBT02 or SBT07 were sterile filtered with Acrodisc units with Mustang E membrane and aliquots snap frozen in liquid nitrogen and then stored at −80°C. Quality control and purity of the isolated SBT02 and SBT07 were assessed by sodium dodecyl sulfate polyacrylamide gel electrophoresis (SDS-PAGE) and immunoblotting. SBT02 was found to be a single band as determined by Coomassie Blue staining, which was confirmed to be SUMO2-positive by western blotting using an anti-SUMO2 rabbit polyclonal antibody (Figure S1). Comparable purity was observed for SBT07 (data not shown).

2.7 | SBT02-FITC labeling

Forty micrograms of SBT02 was dissolved up to 100 µL in borate buffer (pH 9). Fluorescein isothiocyanate (FITC) (#F7250, Sigma) was dissolved in dimethyl sulfoxide (DMSO) to a concentration of 1 µg/µL, added to the SBT02 solution to give a final concentration of 100 ng FITC per 1 µg protein, and immediately mixed under continuous

stirring. The reaction tube was covered with aluminum foil and incubated at RT for 90 min. To remove excess FITC and exchange SBT02 into storage buffer, we used Amicon Ultra-0.5 MWCO 3K centrifugal filter columns (#UFC500324, Millipore), according to the manufacturer's instructions. The collected SBT02 was loaded on SDS-PAGE, and fluorescence was monitored using the ChemiDoc MP Imager (Bio-Rad) with the 488 nm channel.

2.8 | Endothelial permeability of SBT02

Endothelial hCMEC/D3 immortalized cells (Cat. # SCC066, Millipore) were cultured on Corning BioCoat Gelatin Rectangular Canted Neck Culture Flasks w/Vented Cap (CORNING) in MCDB131 medium (Cosmo Bio) containing 10% fetal bovine serum (FBS; SIGMA), 4 ng/mL aFGF (WAKO), 10 ng/mL EGF (WAKO), 50 µg/mL heparin (Gibco Life Technologies), 1 µg/mL hydrocortisone (WAKO Pure Chemical Industries), and 50 µg/mL Gentamicin (Gibco Life Technologies) at 37°C under humidified 5% CO_2. hCMEC/D3 were cultured on Transwell (Cat. no. 3470; pore size 0.4 µm; CORNING) inserts using endothelial basal medium 2 (EBM-2) with an endothelial growth medium 2 (EGM-2) bullet kit containing 2% FBS, antibiotics, and a mixture of growth factors according to the supplier's instructions (LONZA) at 37°C under humidified 5% CO_2. The medium was replaced every 2 days until cells were confluent. The hCMEC/D3 were seeded at 1×10^5 cells/cm^2 and cultured on type I collagen-coated 24-well Transwell inserts. Type I collagen, Cellmatrix, was purchased from SIGMA. Endothelial cell monolayer permeability of SBT02-FITC was evaluated using the permeability marker NaF (MW 376) and bovine serum albumin (BSA)-FITC (MW 67,000) as controls. To initiate the transport experiments, the medium was removed and cells were washed three times with assay buffer (118 mM NaCl, 4.7 mM KCl, 1.3 mM $CaCl_2$, 1.2 mM $MgCl_2$, 1.0 mM NaH_2PO_4, 25 mM $NaHCO_3$, and 11 mM D-glucose, pH 7.4). Assay buffer (1.5 mL) was added to the outside of the insert (abluminal side). Assay buffer (0.5 mL) containing FITC, SBT02, and BSA was loaded on the luminal side of the insert. Samples (0.5 mL) were removed from the abluminal chamber at 60, 90, and 120 min, and immediately replaced with fresh buffer. Aliquots of the abluminal medium were mixed with 200 ll assay buffer, and then the concentration of BSA and SBT02 was determined with a CytoFluor Series 4000 fluorescence multiwell plate reader (PerSeptive Biosystems, Framingham, MA, USA) using a fluorescent filter pair [Ex(k) 485 ± 10 nm; Em(k) 530 ± 12.5 nm]. The permeability coefficients were calculated according to the previously established methodology.[30]

2.9 | Cellular uptake of SBT02 in vivo and immunofluorescence

Five-month old male C57BL/6 mice (Envigo, Bresso, Italy) were used for subcutaneous administration or intrahippocampal injection. Mice were treated once subcutaneously with 40 µg of SBT02-FITC or FITC alone and sacrificed 72 h later as described below. Mice for hippocampal injection were anesthetized with 3% isoflurane in N_2O/O_2 (70%/30%) and maintained with 1.5% to 2% isoflurane in the same gas mixture during the stereotactic surgery. Intrahippocampal injections of 2.5 µg/µL of either SBT02-FITC or FITC alone were performed at the following coordinates: posterior −1.95 mm, lateral ± 1.4 mm, and ventral −2.0 and −1.6 mm (first and second injection site for each hippocampus, respectively). At each injection site, 1 µL of FITC or SBT02-FITC was infused at a rate of 0.5 µL/min, and the needle was left in place for 3 min before withdrawal. Twenty-four hours later mice were perfused with 20 mL of ice-cold PBS 0.1 mol M pH 7.4 followed by 50 mL of chilled paraformaldehyde (4%, PFA) in PBS. Brains were removed from the skull and post-fixed in 4% PFA overnight. The next day, serial coronal sections (30 µm thick) were cut on a vibratome (Leica Biosystems, Wetzlar, Germany). Brain slices were incubated in sodium citrate buffer pH 6.0 (Antigen Decloaker 10x, #CB910 M, Bio Optica) in a heater at 80°C for 30 min. After blocking for 1 h at RT with 5% normal goat serum (NGS, Sigma) in PBS-T (0.3% Triton X-100 in PBS 0.01 M), sections were incubated overnight at 4°C in 5% NGS with 0.3% Triton X-100 in PBS containing rabbit anti-SUMO2 antibody (1:100, #BML-PW9465-0025, ENZO). After washing with PBS, sections were incubated with anti-rabbit Alexa594 secondary antibody (1:500, #A11037, Invitrogen), containing 5% NGS in PBS-T for 1 h at RT. Nuclei were stained with 4',6-diamidino-2-phenylindole (DAPI) (2 µg/mL). Sections were rinsed and coverslipped with ProLong Gold Antifade Mountant (P36930, Invitrogen).

2.10 | Cellular uptake of SBT02 in vitro and immunofluorescence

HEK293 cells exposed to SBT02-FITC (5 µg/mL) or FITC for 24 h were fixed in 4% PFA in PBS for 15 min. Cells were rinsed three times with PBS, permeabilized with 0.5% Triton X-100 for 5 min, and then incubated with blocking solution (3% BSA and 0.2% Triton X-100) for 1 h at RT. The cells were then incubated with the mouse SUMO2 antibody (1:500, # ASM23, Cytoskeleton) overnight at 4°C. After three rinses in PBS, the cells were incubated for 1 h at RT with anti-mouse Alexa594 secondary antibody (1:500, #A11005, Invitrogen) and then washed three more times with PBS. Nuclei were stained with DAPI (2 µg/mL) and the cytoskeleton was labeled with Phalloidin-iFluor 647 Reagent (1:10000, #ab176759, Abcam). After staining, cells were kept in PBS at 4°C until image acquisition. For inhibition studies, HEK293 cells were preincubated with endocytosis inhibitor as follows: chlorpromazine 140 µM for 10 min and dynasore 20 µM for 15 min containing 0.5% DMSO. The same vehicles were used for each control experiment. After removal of the preincubation buffer, the cells were incubated with FITC alone, SBT02-FITC, and transferrin-FITC, in the absence or presence of the inhibitors at 37°C for 60 min.

2.11 | Confocal acquisition

Fluorescent images were acquired using a confocal A1 system (Nikon, Tokyo, Japan) equipped with a confocal scan unit with 405, 488, 561, and 640 nm laser lines with a scanning sequential mode to avoid

bleed-through effects. Three-dimensional images were acquired using a 60 X water immersion objective over a 10- to 12-µm ***z*** axis for cells and 4 µm ***z*** axis for brain slices, with a 0.25 µm step size and final resolution of 0.21 µm/pixel. Cell images were processed using Imaris software (Bitplane) and displayed as volumes or as *x*,*y* single plane images with *z*-projections. Images of brain slices were processed using ImageJ software and displayed as the average intensity of all *z*-planes.

2.12 | Pharmacokinetics of SBT02

Purified SBT02 containing an N-terminal hexa-His tag was administered to wild-type C57BL/6 mice at 20 mg/kg by the subcutaneous and intravenous routes of injection. Plasma and cortex samples were isolated at indicated times over a 24 h period. SBT02 was quantified in plasma and brain using a modified His-tag ELISA (Abcam; ab128573). Brain tissues were homogenized using the Aβ42 ELISA protocol and treated with 5 M urea, and then diluted prior to loading onto the His-tag ELISA plates. Samples were incubated on the capture plates at 4°C overnight and then washed with PBS, and detection was performed using a SUMO2 rabbit polyclonal antibody (dilution 1:200). Standard curves were determined with purified SBT02.

2.13 | Electrophysiological recordings

Electrophysiological recordings were performed as described previously.[31] Briefly, coronal hippocampal slices were cut by a chopper at a thickness of 400 µm and transferred to a recorded chamber where they were allowed to recover for 2 h. During the recovery period and the recording, slices were maintained at 29°C and perfused with artificial cerebrospinal fluid (aCSF) containing NaCl (124.0 mM), KCl (4.4 mM), Na_2HPO_4 (1.0 mM), $NaHCO_3$ (25.0 mM), $CaCl_2$ (2.0 mM), $MgCl_2$ (2.0 mM), and glucose (10.0 mM). aCSF was bubbled with 95% O_2 and 5% CO_2 (flow rate of 2 mL/min). Field excitatory post-synaptic potentials (fEPSPs) were measured after stimulating the Schaffer collateral fibers by a bipolar tungsten electrode placed at CA3 and recording at the *stratum radiatum* of CA1 with a glass pipette filled with aCSF. The input–output curve was generated by plotting the slope of the evoked fEPSP responses at increasing voltages (5–35 V). Baseline was recorded every minute at an intensity eliciting a response ≈35% of the maximum evoked response. After 30 min of stable baseline, LTP was induced through a theta-burst stimulation (4 pulses at 100 Hz, with the bursts repeated at 5 Hz and 3 tetani of 10-burst trains administered at 15-s intervals). Responses were recorded for 2 h after tetanization and measured as the fEPSP slope expressed as percentage of baseline. Results were analyzed in pClamp 11 (Molecular Devices).

2.14 | Behavioral testing

2.14.1 | Fear conditioning

For evaluating associative fear memory, we employed the fear conditioning test, performed on two consecutive days. On the first day the animals were placed in the fear conditioning chamber (33 cm × 20 cm × 22 cm) (Noldus) for 2 min before the presentation of a discrete tone of 2880 Hz at 85 Db (conditional stimulus). In the last 2 s of the tone, mice received a foot shock of 0.8 mA intensity (unconditional stimulus). After the pairing of the two stimuli, mice were left in the chamber for another 30 s in the absence of a stimulus. The second day, mice were returned to the same conditioning chamber for another 5 min without the presence of tone or shock to evaluate contextual fear memory. Freezing behavior, distinguished by the absence of movement except breathing, was monitored during the test using a vision tracking and analysis system (Ethovision XT, Noldus).

2.14.2 | Object location test

For evaluating spatial memory, animals were tested in the object location test. The test was performed as described previously.[32] Briefly, after two consecutive days of habituation in the arena and the objects, the short-term spatial memory was tested. For that, mice were placed in the arena to explore two identical objects positioned in the middle of the arena, having the same predetermined distance from each other. After 1 h, mice were placed back in the arena, where one of the objects was moved in the vertical axis, closer to the wall of the arena. During the 10 min duration of each of the tests, the exploration of the objects was scored manually by a blind observer. The discrimination index was calculated by dividing the difference in exploration time between the two objects during the second trial with the total exploration of the two objects during this trial.

2.15 | Statistical analysis

Experiments were performed in a blinded fashion. Data were expressed as means ± standard error mean (SEM). For electrophysiological recordings, groups were compared by two-way analysis of variance (ANOVA), considering 120 min of recording after tetanus. The last 20 min of each trace was averaged and plotted as residual potentiation. The latter was analyzed by one-way ANOVA followed by Bonferroni's post hoc comparisons. Behavioral experiments were designed in a balanced fashion; for each condition, mice were trained and tested in three to four separate sets of experiments. One-way ANOVA with Bonferroni post hoc correction was used for comparisons among the groups of mice.

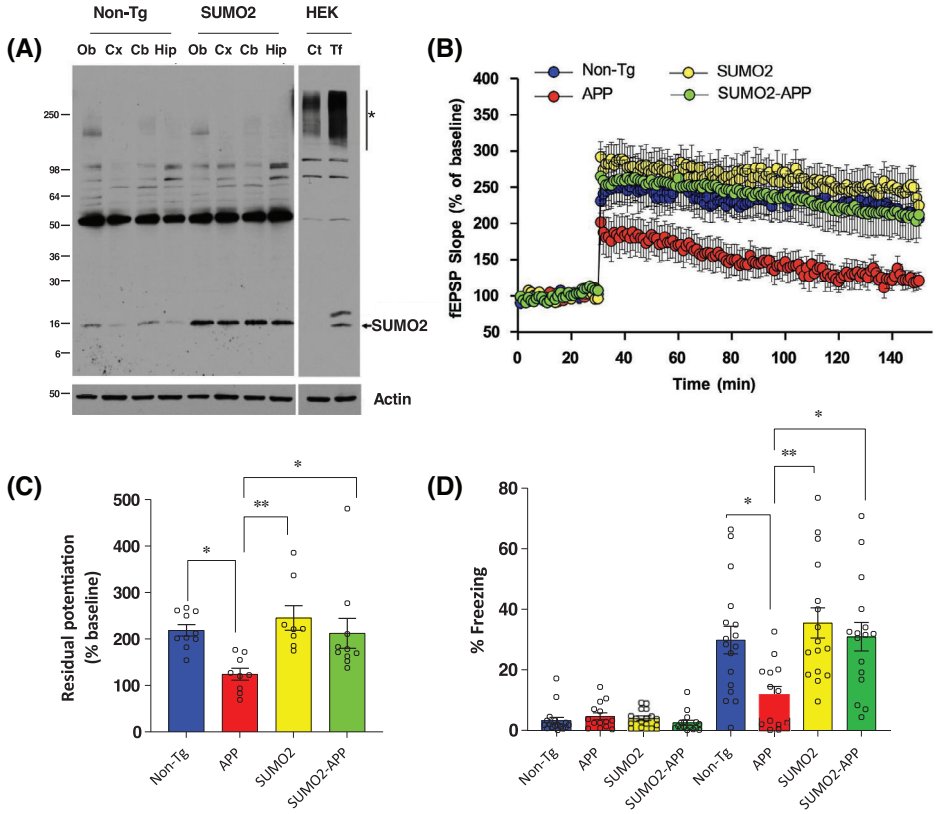

FIGURE 1 Elevated SUMO2 protects against amyloid-induced cognitive decline and defects in synaptic plasticity in vivo. (A) Immunoblot analysis of selected brain regions from transgenic mice expressing human SUMO2 (Ob, Cx, Cb, Hip) showing increased levels of free SUMO2 and no significant increases in high-molecular-weight conjugates. Ct and HA-tagged SUMO2 Tf HEK293 cells were used as positive controls. (B) SUMO2 overexpression protected against LTP impairment of APP mice (two-way ANOVA: Non-Tg vs APP: $F_{(1,17)} = 9.960$, $p = 0.0058$; APP vs SUMO2-APP: $F_{(1,17)} = 5.713$, $p = 0.0287$; APP vs SUMO2: $F_{(1,15)} = 13.91$, $p = 0.002$). (C) fEPSP of the last 20 min of the LTP curve (one-way ANOVA followed by Bonferroni's comparisons: $F_{(3,33)} = 5.107$, $p = 0.0052$; Non-Tg vs APP: $p = 0.0162$; APP vs SUMO2-APP: $p = 0.0272$; APP vs SUMO2: $p = 0.003$). (D) Impairment of associative memory in APP mice measured through contextual fear conditioning was prevented by SUMO2 overexpression with SUMO2-APP transgenics comparable to Non-Tg mice (one-way ANOVA followed by Bonferroni's multiple comparisons: $F_{(3,59)} = 5.153$, $p = 0.0031$; Non-Tg vs APP: $p = 0.018$; APP vs SUMO2 APP: $p = 0.0125$; APP vs SUMO2: $p = 0.0015$). No differences were found in baseline freezing between the different groups (one-way ANOVA for all groups: $F_{(3,59)} = 0.9068$, $p = 0.4433$. $^{**}p < 0.01$; $^{*}p < 0.05$. Data are mean ± SEM. ANOVA, analysis of variance; APP, amyloid precursor protein; Cb, cerebellum; Ct, control untransfected; Cx, cortex; Hip, hippocampus; fEPSP, field excitatory post-synaptic potential; LTP, long-term potentiation; Non-Tg, non-transgenic; Ob, olfactory bulb; SEM, standard error of the mean; SUMO, small ubiquitin modifier; Tf, transfected.

3 | RESULTS

3.1 | *SUMO2* overexpression prevents Alzheimer's disease (AD) synaptic deficits in vivo

To assess its impact on AD pathology, *SUMO2* was genetically elevated in a transgenic mouse model (SUMO2) with expression driven by the prion cos-tet promoter. Elevated free SUMO2 was observed throughout the brain but no substantial elevation in the higher-molecular-weight conjugates was observed (Figure 1A). This is consistent with previous studies, which demonstrated that SUMO2 is relatively quiescent under basal conditions in neuronal cells in vivo, and is activated primarily in response to external cell stress.[33] In vitro, instead, as reported previously, an increase in free SUMO2 and its conjugates was readily observable in HEK293 cells transiently transfected (Tf) with an HA-tagged human SUMO2 (>100 kDa) (Figure 1A). Overexpression of *SUMO2* in the transgenic mouse model at 6 months of age displayed normal LTP, indicating no abnormalities in synaptic function or neurotransmission (Figure S2A,B). Contextual fear conditioning analyses revealed that the SUMO2 transgenics, both homozygous and heterozygous expression, were indistinguishable from Non-Tg controls (Figure S2C). These data indicate that high levels of expression in the *SUMO2* transgene do not result in aberrant conjugation and have no impact on normal neuronal function or learning and memory.

SUMO2 overexpressing mice were crossed with a transgenic mouse model of AD-related amyloid pathology that expresses APP containing the Swedish and Indiana familial AD mutations, also known as the TgCRND8 mouse.[24] TgCRND8 mice have an aggressive pathology timeline due to the high level of Aβ42, leading to amyloid plaque deposition at 3–4 months of age that progresses rapidly to extensive pathology and behavioral deficits. The goal of crossing APP transgenics with homozygous overexpressing SUMO2 mice was to

examine the effects of increased SUMO2 on the AD-related phenotype of amyloid deposition and the accompanying deficits in cognition and synaptic function. Direct comparisons of SUMO2 levels in the various lines did indicate a modest increase in the APP-only transgenics (≈2-fold) over that of the Non-Tgs in 9-month-old animals, possibly due to the increased stress caused by the amyloid load and accompanying neuroinflammation (Figure S3A). As expected, SUMO2 was further increased in the SUMO2-APP transgenics (≈4-fold), which was similar to that of the heterozygous SUMO2 transgenics, whereas much higher free SUMO2 was observed in the homozygous mice. This was confirmed by additional quantitative analysis of the APP and SUMO2-APP lines (n = 4), where a 2-fold increase in SUMO2 was observed for the double transgenics (Figure S3B,C). The SUMO2-APP double transgenics were examined at 9 months of age when the amyloid plaque load is extensive and representative of late-stage disease. Electrophysiological studies confirmed previous reports where the APP transgenics exhibited significant LTP impairment when compared to Non-Tg animals (Figure 1B,C). In contrast, although the SUMO2 transgenic mice behaved similarly to Non-Tg mice, increased *SUMO2* expression in the APP mice was capable of preventing the LTP impairment in SUMO2-APP as compared to mice expressing just the *APP* transgene (Figure 1B,C). The protective action of SUMO2 in LTP was confirmed in learning and memory assessments, where APP transgenic mice exhibited significant cognitive dysfunction, whereas SUMO2-APP transgenic mice performed similarly to Non-Tg animals (Figure 1D). Therefore, the synaptic and cognitive functions in the SUMO2-APP double transgenics were effectively the same as Non-Tg animals, indicating a neuroprotective effect against amyloid toxicity conferred to the mice by increased cellular SUMO2.

Given that SUMOylation has been implicated in Aβ processing, we tested whether an increase in SUMO2 could alter the levels of soluble and insoluble Aβ as well as amyloid plaques. Immunocytochemistry for Aβ indicated that the typical distribution and expected density of plaques within the hippocampus and cortex were comparable in the APP and SUMO2-APP transgenics (Figure 2A). Quantitative image analysis of the plaque areas demonstrated no significant differences in the dense plaque cores or the diffuse halos surrounding plaques (Figure 2B). Fractionation and quantification of the soluble and insoluble Aβ42 in the cortex and hippocampus (C/H) and Cb indicated no significant differences in APP and SUMO2-APP transgenics (Figure 2C). A potential mechanism of action for the preservation of LTP and cognition is the increase in SUMO2 conjugation of synaptic proteins. In fact, we observed an increase in SUMO2 in isolated synaptosomes (Figure 2D). The synaptic trafficking of SUMO2 in the transgenics was examined further with synaptosomes isolated from Non-Tg and *SUMO2* overexpressing mice. The synaptosome isolation was monitored and confirmed by the enrichment of Homer1 in both the crude and purified synaptosomal fractions (Figure S4A). Total brain lysates probed for SUMO2 indicated an ≈4-fold increase for the unconjugated SUMO2 in the transgenic animals as compared to wild-type, Non-Tg controls (Figure S4B,E. SUMO2 was further elevated to ≈7-fold in the crude synaptosomal fraction (Figure S4C,F) and to ≈12-fold in the purified synaptosomes (Figure S4D,G). These data support the increase of SUMO2 in synaptic compartments and link to a potential mechanism of action.

Consistent with the Aβ levels, *SUMO2* overexpression had no effect on amyloid processing, as immunoblotting for APP full-length and C-terminal fragments was equivalent in the APP and SUMO2-APP transgenic mice (Figure S5A). Quantitation of the sAPPβ/Sw fragment was also comparable, confirming that *SUMO2* overexpression did not impact secretase activity (Figure S5B). This was equally the case for murine Aβ42, where ELISA-based assessments confirmed similar levels in both the Non-Tg and the SUMO2 transgenic mice, indicating normal processing of endogenous APP (Figure S5C). These data indicate that SUMOylation is a significant regulator of neuronal pathways, and that the specific enhancement of SUMO2 levels and its subsequent conjugation may be beneficial for the treatment of AD amyloid pathology. To this end, a recombinant biologic, SBT02, was developed that mimics SUMO2 activity, and its therapeutic efficacy was investigated in the model of AD amyloid pathology.

3.2 | SUMO2 biologic pharmacokinetics and bioavailability

A possible pharmacologic approach to increase SUMO2 conjugation when it is reduced, as is the case in AD brains, is to provide additional SUMO2 capable of reaching the brain parenchyma.[34] Consequently, we tested whether recombinant SUMO2 analogue administrated peripherally was capable of reaching the brain and exhibited functional conjugation to target proteins. The cell permeability of SBT02 was initially examined in vitro using an FITC-labeled version of the purified recombinant protein (Figure S6). Immunofluorescence microscopy revealed that exogenously applied SBT02-FITC (1 µg/mL) was taken up by HEK293 cells, which was confirmed by double-labeling with phalloidin, whereas no signal was observed for FITC alone (Figure S6A). Examination of confocal sectioning (z-stacks) through cells incubated with exogenous FITC-labeled SBT02 showed co-localization with SUMO2 immunofluorescence and its distribution throughout the cytoplasmic and nuclear compartments (Figure S6B). Internalization of SBT02-FITC was reduced significantly in the presence of dynasore and chlorpromazine, which inhibit endocytosis (Figure S6C). Cell uptake of SBT02 was confirmed in a model of the blood–brain barrier that utilizes human endothelial cell monolayers. Application of SBT02 indicated that the protein traversed the endothelial cell layer as determined by fluorescence assay of aliquots taken from the transwell after 1–2 h incubation (Figure S6D). In addition, SBT02 was administered to HEK293 cells in culture, which demonstrated uptake and active conjugation to target proteins at 24 h (Figure S6E). These data cumulatively support the efficient uptake and cytoplasmic internalization of SBT02. SBT02 uptake in brain cells was confirmed by immunohistochemical analyses of SBT02-FITC administered intracerebrally and peripherally (Figure S7). Cumulatively, these data demonstrate that SBT02 is readily taken up by cells in vitro and also in vivo by peripheral subcutaneous (SQ) administration.

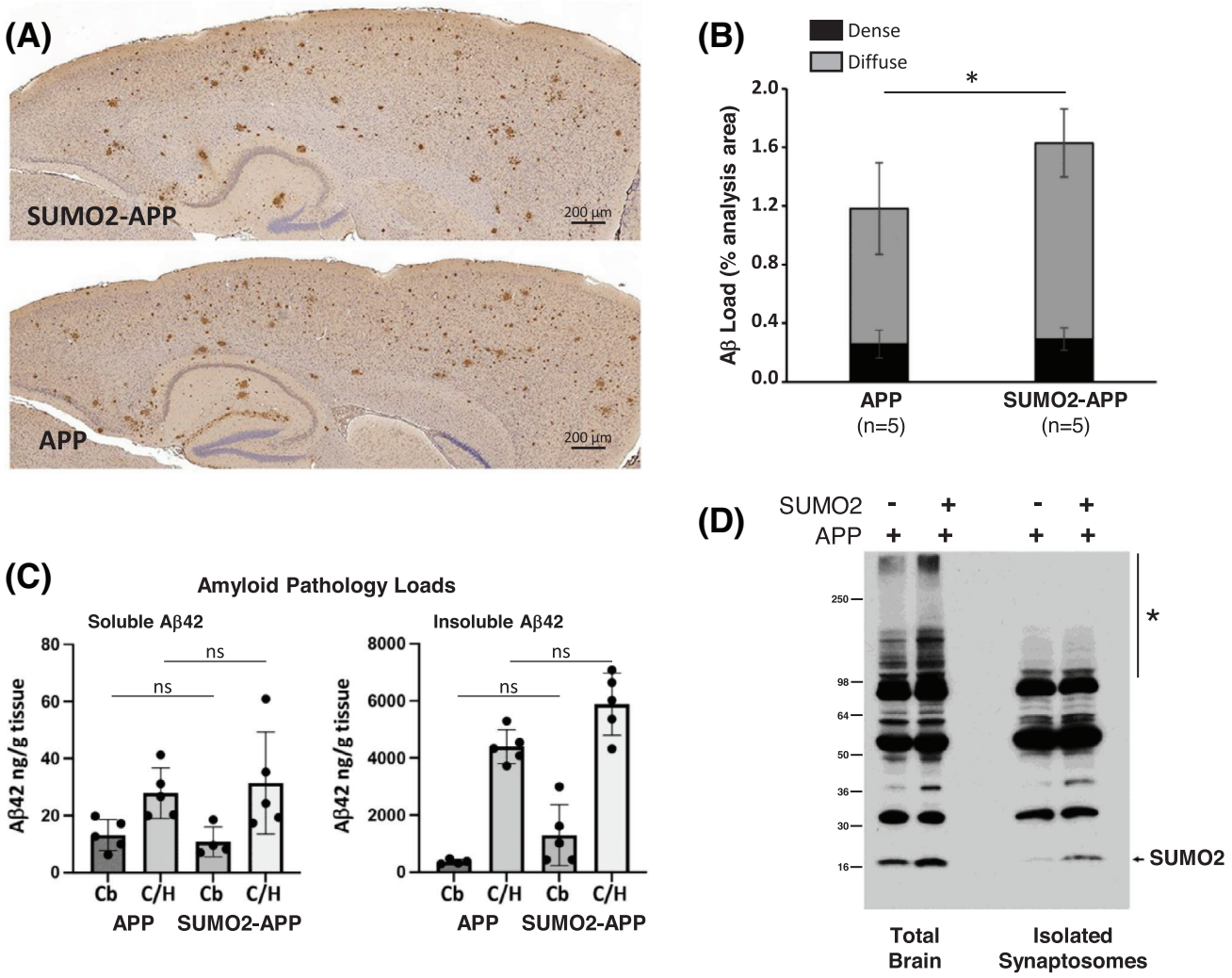

FIGURE 2 Amyloid loads and SUMO2 distribution in brain. (A) Representative images showing amyloid immunohistochemistry in the APP and SUMO2-APP transgenics displaying comparable plaque densities. (B) Quantitative image analysis of amyloid plaques revealed comparable levels in APP and SUMO2-APP transgenic mice indicating that SUMO2 overexpression had no effect on the amounts of dense plaques (*black*) and diffuse (*gray*) amyloid deposits, which were modestly increased in the SUMO2-APP mice (*$p < 0.05$; Tukey's multiple comparisons test after one-way ANOVA). (C) Quantification of soluble and insoluble Aβ42 as determined by sandwich ELISA indicated no significant difference in the Cb and C/H extracts; ns, Dunnett's multiple comparison test after one-way ANOVA. (D) Immunoblotting for SUMO2 demonstrated an increase in SUMO2 higher-molecular-weight conjugated proteins (*) in the SUMO2-APP transgenics and elevated free SUMO2 in synaptic compartments in SUMO2-APP transgenics as compared to APP mice. Elevated SUMO2 was also observed in isolated synaptosomes suggesting a targeting to synapses and potential impact on activity. Aβ, amyloid beta; ANOVA, analysis of variance; APP, amyloid precursor protein; Cb, cerebellum; C/H, cortex-hippocampus; ELISA, enzyme-linked immunosorbent assay; ns, not significant; SUMO, small ubiquitin modifier.

Distribution and bioavailability of SBT02 in the plasma and brain were determined by ELISA for a His-tagged version of the SUMO2 recombinant protein. SBT02 levels in mice following intravenous (IV) injection were maximal at ≈30 min in plasma, and no detectable levels were observed at 4 h (Figure 3A). In contrast, SQ injection resulted in a peak for SBT02 at ≈1 h, with levels that were still detectable at 4 h (Figure 3B). Brain levels for SBT02 by IV administration correlated with a slow increase over the course of 4 h and reached a maxima of 50 ng/g at 24 h (Figure 3C). The levels of IV administered SBT02 were decreased at 48 h and were undetectable at the 72 h mark. SQ administration was equally effective at brain penetration, with significant levels observed at 15 min that were comparable to 4 h post-injection (Figure 3D). In addition, SQ administration resulted in the maintenance of high SBT02 brain concentrations for up to 24 h; a maximum concentration of ≈250 ng/g was reached at 72 h and the level remained high even at 120 h post-administration (Figure 3D). These findings indicate that SQ injections of SBT02 exhibit a long half-life that may require only a single weekly dosing.

3.3 | SBT02 toxicology and pathology assessments

Initial toxicology studies were conducted with an acute administration of 100 mg/kg or 300 mg/kg over the course of 7 days and a

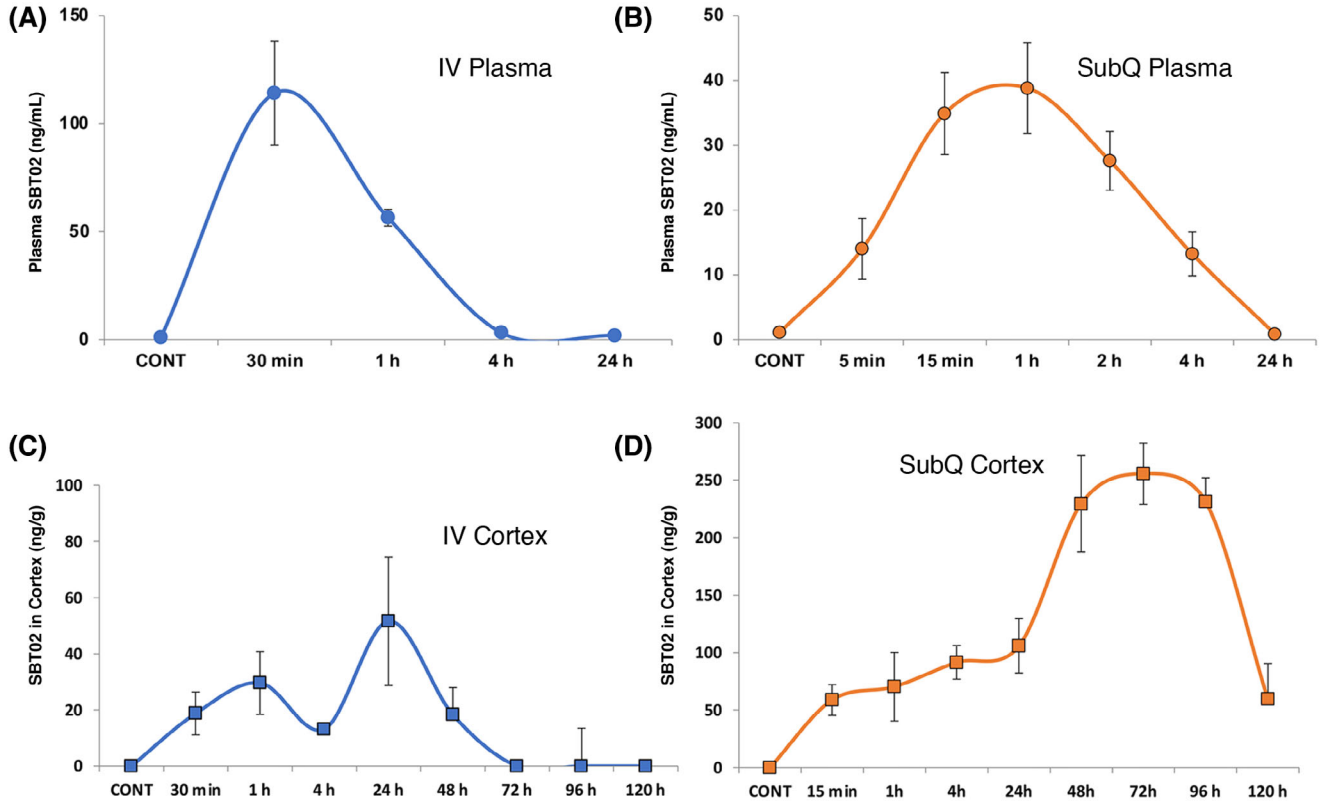

FIGURE 3 Pharmacokinetics of the active SUMO2 biologic. SBT02 levels were examined following IV or SubQ administration. Wild-type C57BL/6 mice were administered a single injection of N-terminally His-tagged SBT02 (20 mg/kg), and samples were analyzed at various time points. (A) Quantification of the plasma using His-ELISA assays showed a rapid elevation in SBT02 following IV injection that peaked at ≈30 min and was completely cleared from the periphery after 4 h. (B) SubQ injected SBT02 peaked at 1 h and gradually decreased with detectable levels of ≈15 ng/mL at 4 h post-injection. Peak plasma levels were higher in the IV-injected group at ≈115 ng/mL as compared to SubQ injected mice at ≈40 ng/mL plasma, indicating that IV administered SBT02 results in higher plasma concentrations but these are reduced more rapidly than in mice receiving SubQ-injected biologic. (C) SBT02 concentrations in the cortex following IV administration gradually increased and reached a maximum of ≈60 ng/g tissue 24 h post-injection. (D) SubQ-injected SBT02 rapidly increased in the cortex and reached a maximal level of ≈125 ng/g tissue at the 4 h time point, and significant levels were observed 120 h post-injection. $n = 3$ mice per time point, and data are mean ± SEM. ELISA, enzyme-linked immunosorbent assay; IV, intravenous; SEM, standard error of the mean; SubQ, subcutaneous; SUMO, small ubiquitin like modifier.

subchronic administration of 100 mg/kg for 15 days. Analysis of body and tissue weights indicated that SBT02 had no adverse effects for either the acute or subchronic treatments relative to the saline-treated controls (Table S1). However, increases in spleen and kidney weights were observed in mice receiving the acute doses of 300 mg/kg. Clinical chemistry analysis confirmed that the liver and kidney function was largely normal following the acute or subchronic dosing (Table S2). The only statistically significant changes were in male mice receiving the acute 100 mg/kg (7 days), which had higher levels of cholesterol, high-density lipoprotein (HDL), and triglycerides as compared to female mice, and a reduction in low-density lipoprotein (LDL). Clinical pathology was also conducted on APP and Non-Tg mice treated with SBT02 or saline (100 mg/kg; 7 days), and SBT02 was found to have no major impact on the gross pathology of multiple organ tissues (brain, heart, liver, kidney, spleen; Table S3). These pharmacokinetic and toxicology investigations are consistent with a high brain bioavailability of SBT02, and the biologic is well tolerated at high doses.

3.4 | SBT02 prevention of cognitive and LTP impairments

Testing was conducted to examine the ability of SBT02 to intervene in a prophylactic paradigm when cognitive function is still normal and amyloid pathology corresponded to the equivalent of early-stage deposition. To assess prophylactic efficacy, a cohort of APP transgenic mice was treated with the active SBT02 beginning at 3 months of age prior to the onset of amyloid accumulation (pre-pathology) and they were cognitively normal (Figure 4A). Individual groups of APP transgenics were administered: (1) the active SBT02; (2) an inactive form of the SUMO2 biologic, SBT07; or (3) saline. SBT07 was a mutated form of the biologic that lacked the C-terminal di-glycine motif necessary for conjugation to target proteins. Non-Tg animals receiving comparable treatments were used as controls. SBT02 and SBT07 (20 mg/kg) were administered three times/week for 3 months. Animals were assessed for behavior and synaptic function at the 6-month

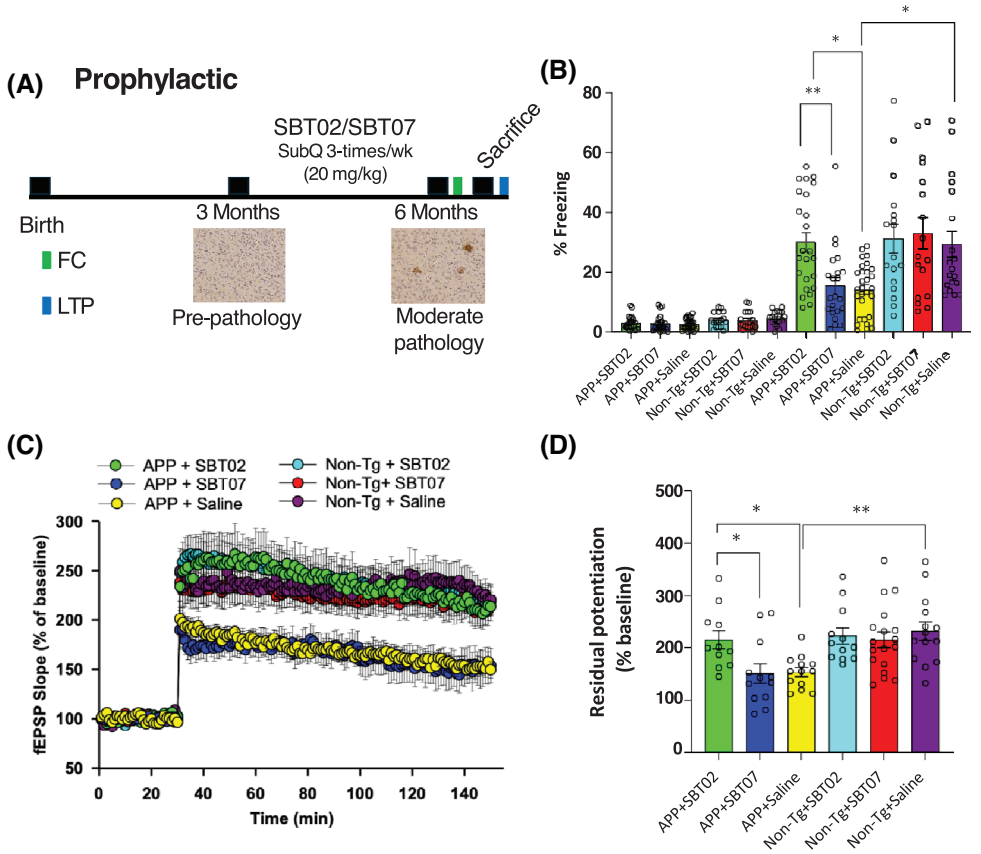

FIGURE 4 Recombinant biologic, SBT02, mimicking SUMO2 activity prevents impairments in synaptic and cognitive function. (A) Schematic of the prophylactic therapy time course for treatments with SUMO2 biologics. (B) APP mice exhibit LTP deficits in comparison to littermates, Non-Tg mice ($F_{(1,25)} = 11.66$; $p = 0.0022$). SBT02 prevented the LTP impairment in APP mice as compared to inactive SBT07 ($F_{(1,21)} = 7.662$; $p = 0.0115$) or saline ($F_{(1,22)} = 10.19$; $p = 0.042$) and exhibited potentiation similar to that of Non-Tg mice receiving comparable treatments ($F_{(1,21)} = 0.006$; $p = 0.9401$). (C) fEPSP of the last 20 min (one-way ANOVA followed by Bonferroni's multiple comparisons: $F_{(5,74)} = 5.06$, $p = 0.0005$; APP + saline vs Non-Tg + saline: $p = 0.0021$; APP + SBT02 vs APP + SBT07: $p = 0.028$; APP + SBT02 vs APP + saline: $p = 0.0328$). (D) Deficit in associative memory as determined by contextual fear conditioning was prevented by SBT02 administration as compared to SBT07- or saline-treated APP animals (one-way ANOVA followed by Bonferroni's multiple comparisons: $F_{(5,120)} = 5.940$, $p < 0.0001$; APP + saline vs Non-Tg + saline: $p = 0.0353$; APP + SBT02 vs APP + SBT07: $p = 0.012$; APP + SBT02 vs APP + saline: $p = 0.002$). No differences were found in baseline freezing between the different groups (one-way ANOVA for all groups: $F_{(5,120)} = 2.186$, $p = 0.06$). $^{**}p < 0.01$; $^{*}p < 0.05$. Data are mean ± SEM. ANOVA, analysis of variance; APP, amyloid precursor protein; fEPSP, field excitatory post-synaptic potential; LTP, long-term potentiation; Non-Tg, non-transgenic; SUMO, small ubiquitin modifier.

time point when amyloid pathology had developed with a moderate phenotype.

Electrophysiological examination demonstrated that SBT02 was able to prevent the onset of synaptic dysfunction. The treated APP transgenic animals exhibited synaptic plasticity (measured through LTP) and basal synaptic transmission (measured through the input–output relationship) similar to that of Non-Tg mice receiving the identical dosing (Figures 4B,C and S8a). APP transgenic mice that received inactive SBT07 or saline exhibited the anticipated impairment in LTP and basal synaptic transmission (Figures 4B,C and S8a). No changes were observed in Non-Tg mice that underwent a similar treatment regimen. The ability of SBT02 to preserve normal synaptic transmission was similarly reflected in contextual fear conditioning (Figure 4D). APP transgenic mice receiving SBT02 maintained their cognitive abilities and were not significantly different from the Non-Tg animals. Similar to fear conditioning, SBT02 was able to prevent short-term memory impairments observed in the saline-treated APP transgenic mice tested in the object location test (Figure S9A), while the SBT07 treatment did not improve the memory defects typical of APP transgenic mice and the associated amyloid pathology.

As with the SUMO2-APP animals, treatment with the SBT02 biologic did not alter the underlying amyloid pathology, as determined by Aβ immunohistochemistry (Figure 5A). Image analysis and quantification of plaque areas confirmed these findings, with the dense and diffuse amyloid deposits showing no statistical differences in the SBT02-, SBT07-, or saline-treated animals (Figure 5B). Quantification of the soluble (monomeric and oligomeric) Aβ42 and the insoluble, plaque-associated Aβ42 in extracts from the combined cortex and hippocampus were also comparable for all groups of treated mice, which supported the lack of an impact of SBT02 treatment on amyloid pathology or processing (Figure 5C). Similar analyses of the soluble and insoluble amyloid in dissected cortices and olfactory

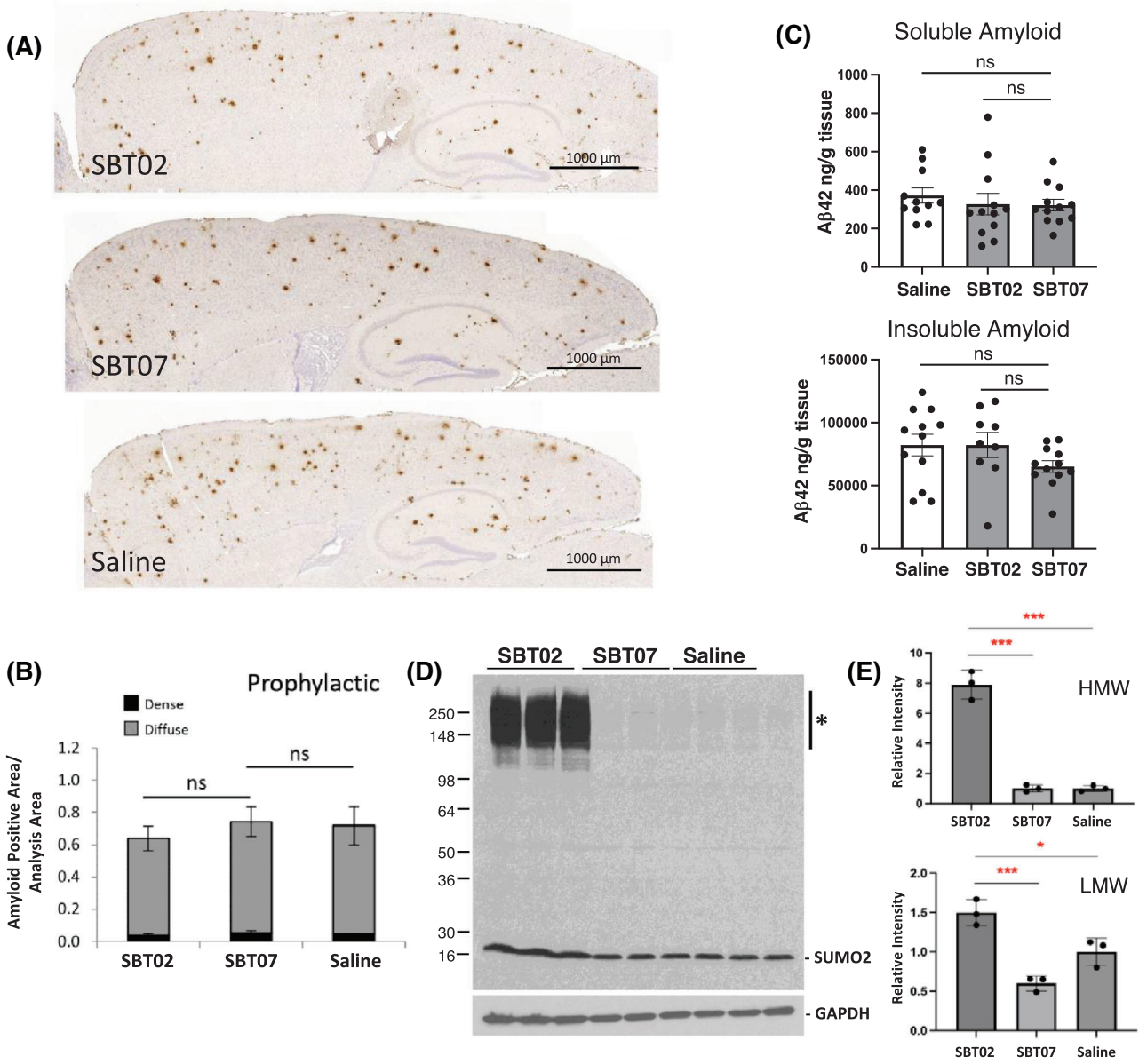

FIGURE 5 Amyloid loads and SUMO conjugation in treated APP transgenics. Representative immunocytochemistry images for the prophylactic treatments showing (A) similar plaque densities in APP mice treated with SBT02, SBT07, or saline. Sections were stained for Aβ, indicating comparable amyloid plaque loads in the cortex and hippocampus. Amyloid plaque loads were assessed by immunohistochemistry and image analysis of the cortex and hippocampus. (B) Dense plaque cores (*black*) and diffuse halos (*gray*) for APP-Tg mice treated prophylactically and examined at the 6-month end point ($n = 3$; 5 sections/animal) or (C) ELISA quantification of soluble and insoluble Aβ42 in cortex-hippocampus indicated; ns, Tukey's multiple comparisons after one-way ANOVA. (D) SUMO2 immunoblotting revealed an increase in HMW conjugates (*) and free SUMO2-positive bands for whole brain homogenates from SBT02-treated APP transgenics relative to SBT07- and saline-treated mice. (E) Quantification of the SUMO2 immunoreactivity indicated an ≈8-fold increase in HMW SUMO2-positive conjugates in animals that received SBT02 from 3 months of age until being sacrificed at 6 months (prevention therapy); the LMW free SUMO2 was also elevated in the SBT02 animals consistent with the treatment. Data are mean ± SEM, *; $p < 0.05$, ***; $p < 0.001$ by Tukey's multiple comparison test following ordinary one-way ANOVA. Aβ, amyloid beta; ANOVA, analysis of variance; APP, amyloid precursor protein; ELISA, enzyme-linked immunosorbent assay; HMW, high molecular weight; LMW, low molecular weight; ns, not significant; SEM, standard error of the mean; SUMO, small ubiquitin like modifier.

bulbs (Obs) also remained unaffected by the treatment (Figure S10). These data support the conclusion that the prevention of cognitive and synaptic deficits by SBT02 did not result from a reduction in Aβ oligomers (Aβos) or overall amyloid pathology. The most marked change in the APP transgenics treated with SBT02 was an increase in the amount of free and high-molecular-weight (HMW) SUMO2-positive conjugated proteins, which was not observed in the SBT07- or saline-treated mice (Figure 5D). Quantification of the higher-molecular-weight SUMO2-reactive conjugates indicated an ≈8-fold increase in the SBT02-treated APP transgenics (Figure 5E). To confirm that the observed conjugates were due to SBT02 modifications, brain homogenates from treated APP transgenics were used for Ni-

affinity chromatography to isolate the His-tagged SBT02 and any conjugated proteins. Homogenates from SBT02- or saline-treated APP transgenics from the prevention study were denatured in guanidinium hydrochloride to expose the hexa-His domain, and SBT02 was isolated using Ni-NTA agarose beads. Immunoblotting of the eluates from the Ni-pulldown probed for SUMO2 demonstrated that the HMW conjugates were due exclusively to SBT02 modification of target proteins (Figure S11). Therefore, it is likely that the modification of neuronal and synaptic proteins by the peripherally administered SBT02 biologic was responsible for mitigating the Aβo synaptotoxicity in the APP transgenics.

3.5 | SBT02 reversal of AD-related cognitive and synaptic impairments

For reversal of late-stage AD, treatments were initiated in APP transgenic mice beginning at 6 months of age when amyloid pathology was moderate and LTP and cognitive deficits were observed (Figure 6A). This was equivalent to the degree of impairment associated at the endpoint for the prophylactic study (see Figure 4). SBT02 was administered for 3 months and mice were assessed for cognitive and synaptic function at 9 months of age when the amyloid pathology was severe and corresponded to late-stage AD. Control groups were APP transgenics administered by SQ injections of SBT02, SBT07, or saline and compared to Non-Tg mice receiving the same treatments. Although the APP transgenics were treated when impairments were already well established, it was found that SBT02 was able to reverse the LTP (Figure 6B,C) and basal synaptic transmission (Figure S8b), deficits that were indistinguishable from Non-Tg animals. Comparable effects on reversing the phenotype were observed for cognitive assessments, where SBT02 restored normal learning and memory as determined by fear conditioning (Figure 6D) and the object location test (Figure S9b) at the 9-month endpoint. In contrast, APP transgenics that were administered SBT07 or saline continued to decline further with respect to their performance on the fear conditioning testing.

Consistent with the prevention study, immunocytochemistry of the cortex and hippocampus of SBT02-, SBT07-, or saline-treated APP transgenics indicated extensive Aβ-positive accumulations of comparable densities (Figure 7A). This was supported by image analysis, which indicated no quantifiable differences in dense or diffuse amyloid plaque deposits (Figure 7B). Fractionation and quantification of the insoluble Aβ42 levels from the cortex, Ob, and Cb from treated animals further confirmed the lack of an impact on amyloid loads in the groups of treated APP mice (Figure S12). The one exception was the insoluble Aβ42 in the cortices of the SBT02- and SBT07-treated animals, which exhibited elevated levels relative to the saline-treated mice (Figure S12B). A similar analysis of the soluble Aβ42 levels indicated no changes in the Ob or Cb, whereas a slight increase occurred in the cortices of SBT02-treated mice as compared to those receiving SBT07 (Figure S12A).

Unlike many amyloid-based therapeutics, the SBT02 biologic does not enhance the clearance of Aβ or reduce its production by altering amyloid processing. In agreement with our original hypothesis, SBT02 administration for prevention and reversal trials increased the levels of free SUMO2 and enhanced conjugation in the brain (Figure 7C). Based on quantification of the immunoblots, the free, SUMO2-positive monomers were modestly increased by 30%–40% in the SBT02-treated mice, whereas the HMW conjugates were 3-fold higher as compared to the SBT07- and saline-treated animals (Figure 7D). These SUMO2-positive conjugates are currently under investigation, and we anticipate that numerous target proteins will be identified rather than a single effector of SBT02 activity, which is in keeping with previous reports.[35–37] Consistent with this possibility, the outcome of the enhanced SUMO2 conjugation appears to be an increase in synaptic density and/or stability. This is illustrated by the elevated levels of the post-synaptic PSD-95 and Homer1 and presynaptic synaptophysin in the APP mice from the reversal study (Figure 8). Quantification of PSD-95 and Homer1 levels from a subset of animals demonstrated an increase in SBT02-treated animals (Figure 8B,D). A similar elevation in synaptophysin was also observed in the APP transgenics treated with SBT02 (Figure 8F). Examination of the different mouse lines indicated that there were no major variations in PSD-95 as a result of background strains and confirmed the effects of SBT02 treatment (Figure S13). Although the APP transgenics have extensive, late-stage amyloid pathology and synaptotoxicity mediated by Aβos, the increase in these synaptic markers demonstrated the beneficial effects of SBT02 against dysfunction and/or damaged synapses caused by amyloid toxicity.

4 | DISCUSSION

Cumulatively, the findings of this investigation have shown that administration of this SUMO2-based biologic results in the prevention and reversal of synaptic and cognitive deficits associated with mild and moderate AD. Moreover, administration of a SUMO2-based biologic also results in the reversal of synaptic and cognitive deficits associated with mild and moderate AD. SBT02 treatment has no impact on the extent of amyloid pathology but likely acts by counteracting the toxic effects of Aβ that are responsible for synaptic loss and dysfunction. These data suggest that SBT02 acts downstream of the Aβ-mediated synaptotoxicity, and several intriguing possibilities present themselves for a potential mechanism of action related to mGluR subtypes and AMPA receptors (AMPARs) that are linked to SUMO2 and Aβ toxicity.[38–43]

We found that basal neurotransmission was impaired in APP mice, and treatment with SBT02 was able to ameliorate these impairments in both groups, with SBT02-treated APP mice exhibiting similar basal neuronal transmission to that of Non-Tg mice. These findings suggest that the synaptic connectivity in the CA3–CA1 area was compromised in the APP mice. It is important to note that chronic treatment with SBT02 was able to reverse the synaptic function at the Schaffer collateral synapses. The impaired synaptic function could be attributed to synaptic loss and/or defects in neuronal communication, such as impaired release of neurotransmitters from the presynaptic neurons or decrease in the number of post-synaptic receptors. Indeed, pre-

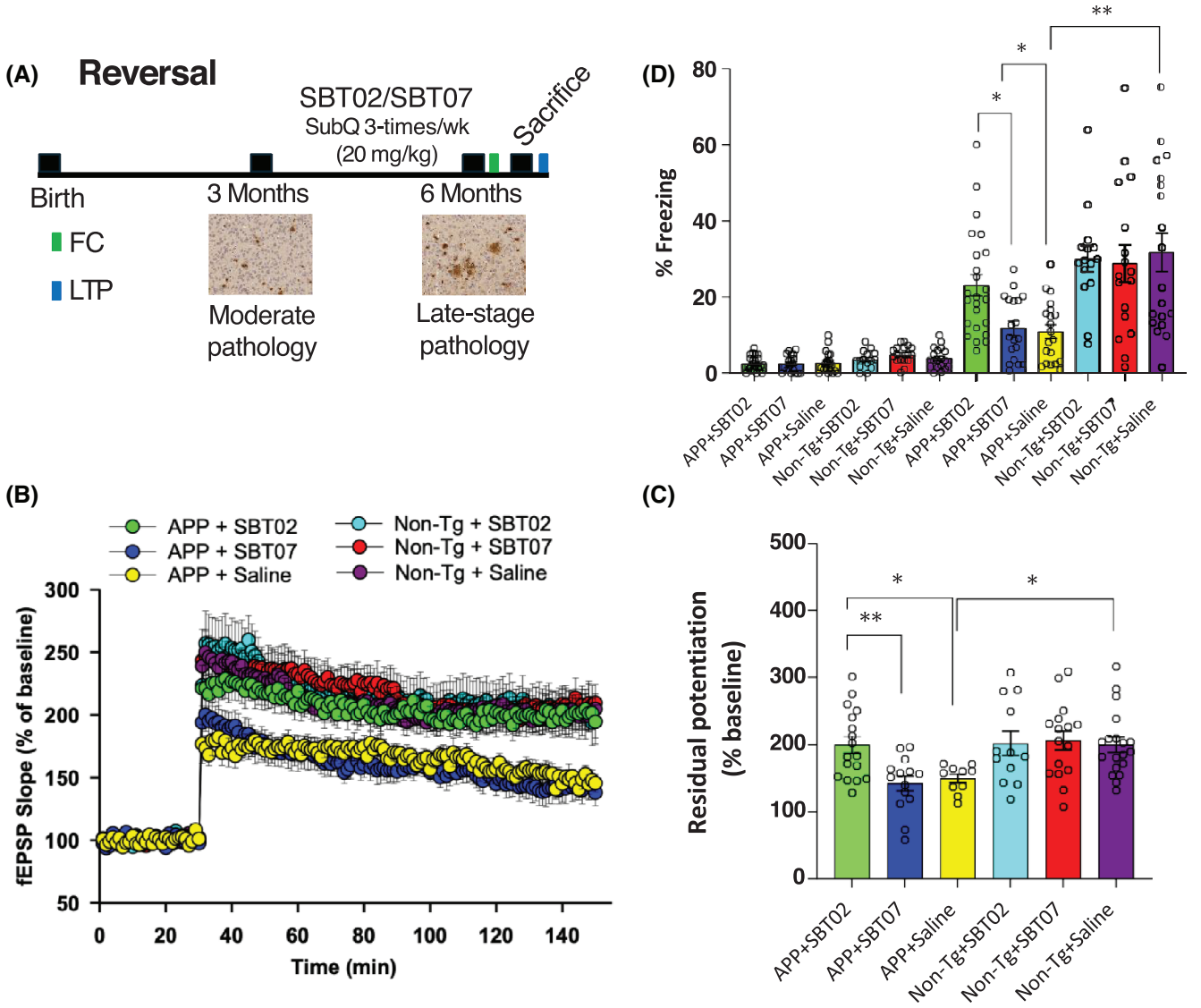

FIGURE 6 SBT02 reverses cognitive and synaptic impairments in late-stage disease. (A) Timelines for the reversal study with SBT02/SBT07 and treatment of APP transgenics with pre-existing amyloid pathology and LTP/cognitive impairments at 6 months (moderate amyloid load) until 9 months of age (severe amyloid load). (B) LTP impairment in APP mice (APP + saline vs Non-Tg + saline: $F_{(1,27)} = 8.138$, $p = 0.0082$) was reverted by SBT02 treatment as compared to animals receiving inactive SBT07 ($F_{(1,29)} = 11.16$; $p = 0.0023$) or saline ($F_{(1,25)} = 7.433$; $p = 0.0082$), and exhibited potentiation similar to that of Non-Tg mice receiving comparable treatments ($F_{(1,27)} = 0.3956$, $p = 0.5347$). (C) fEPSP of the last 20 min (one-way ANOVA followed by Bonferroni's multiple comparisons: $F_{(5,82)} = 4.638$, $p = 0.0009$; APP + saline vs Non-Tg + saline: $p = 0.0328$; APP + SBT02 vs APP + SBT07: $p = 0.0054$; APP + SBT02 vs APP + saline: $p = 0.0381$). (D) Associative memory deficits in APP mice (APP + saline vs Non-Tg + saline: $p = 0.002$), assessed by contextual fear conditioning were reversed by SBT02 relative to transgenics treated with SBT07 ($p = 0.037$) or saline ($p = 0.02$) (one-way ANOVA for all groups: $F_{(5,98)} = 7.183$, $p < 0.0001$. No difference was found in baseline activity (one-way ANOVA for all groups: $F_{(5,98)} = 1.719$, $p = 0.137$). $^{**}p < 0.01$; $^{*}p < 0.05$. Data are mean ± SEM. ANOVA, analysis of variance; APP, amyloid precursor protein; fEPSP, field excitatory post-synaptic potential; LTP, long-term potentiation; Non-Tg, non-transgenic; SEM, standard error of the mean.

vious work has shown that APP mice exhibit neuronal loss in the hippocampus, accompanied by reduced levels of GluN1-NMDARs and GluA2-AMPARs, starting at 3 months of age.[44] Another group reported decreased levels of the presynaptic marker synaptophysin in young, 2-month-old APP mice. The downregulation of synaptophysin was correlated with loss of synapses.[45] Although our study does not provide direct evidence on the number of synapses and their morphology, the apparent role of SUMOylation in regulating trafficking of AMPARs, as well as our findings showing restored levels of synaptic markers (PSD-95, Homer1, and synaptophysin), suggest that treatment with the SUMO2-mimetic compound is able to prevent and restore loss of functional synapses, leading to intact synaptic transmission and cognitive function.

AMPARs have critical roles in LTP and long-term depression (LTD), and their synaptic biology is linked to SUMOylation. This has been reported through the observations that the expression of the SENP1 catalytic domain or a dominant-negative Ubc9 is able to block LTP.[46] Although the AMPARs themselves have not been shown to be modified

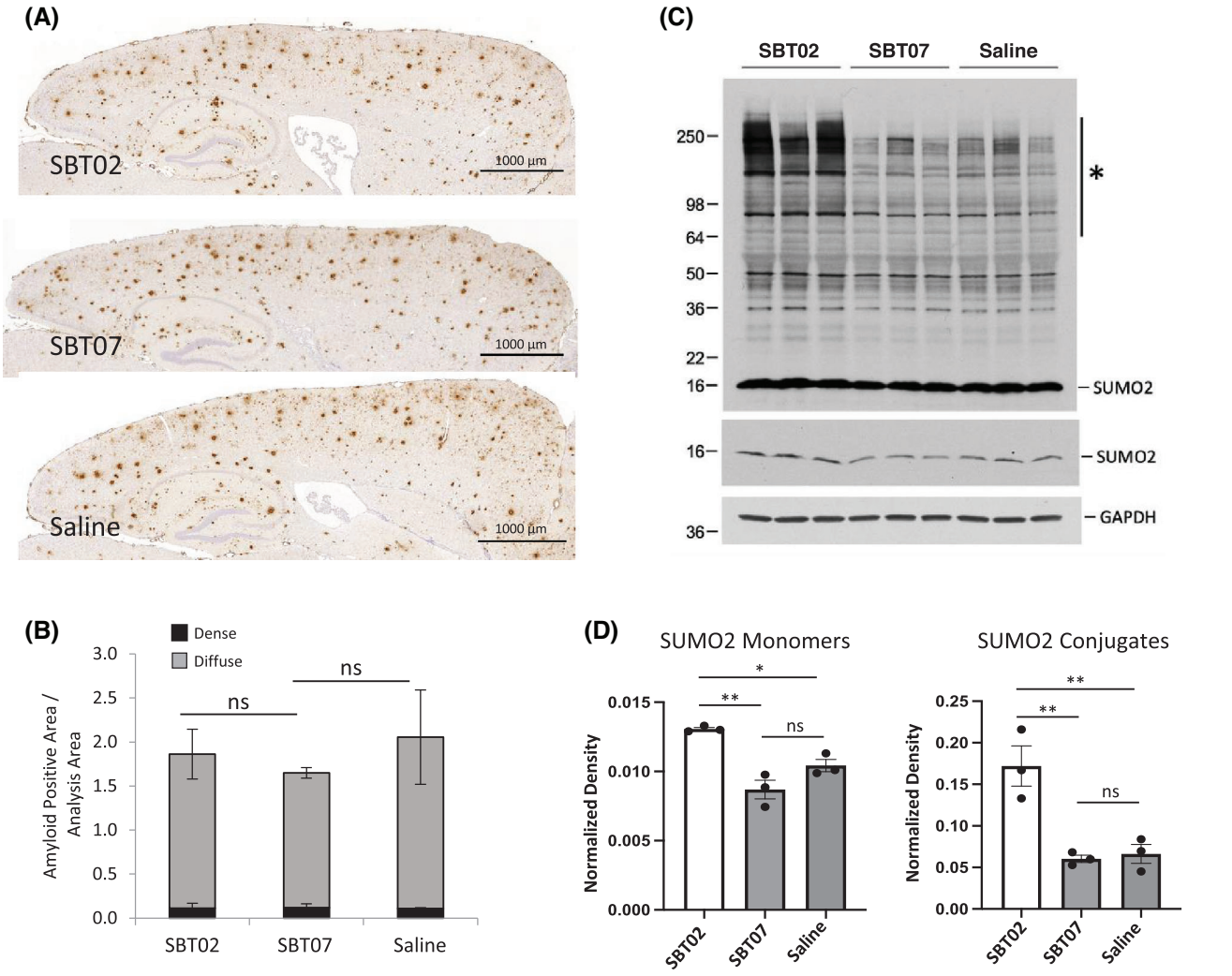

FIGURE 7 Amyloid loads and SUMO2 conjugation in the reversal treatment. (A) Representative immunocytochemistry images for the reversal mice showing comparable plaque densities in APP transgenes treated with SBT02, SBT07, or saline. (B) Quantitative image analysis of the cortex and hippocampus indicated no changes in dense plaque cores (*black*) or diffuse halos (*gray*) for APP-Tg mice examined at the late stage of pathology (9 months of age; $n = 3$; five sections/animal) receiving the active SBT02, inactive SBT07, or saline (Tukey's multiple comparisons test after one-way ANOVA, ns). (C) Immunoblot indicating the increase in SUMO2-positive conjugates and monomers in the SBT02-treated animals. (D) Quantification of the free and conjugated SUMO2-positive proteins. ANOVA, analysis of variance; APP, amyloid precursor protein; ns, not significant; SUMO, small ubiquitin like modifier; Tg, transgenic.

directly, SUMOylation has been shown to regulate AMPAR trafficking to the plasma membrane during LTP, which may be facilitated by the intermediaries such as the Arc protein. Arc is directly modified by SUMO1, and mutant Arc lacking the SUMOylation sites is unable to regulate the LTP-dependent recycling of AMPARs from the synaptic membrane.[39] AMPARs are also linked to amyloid pathology, in that Aβos promote the removal of AMPARs from the synaptic membrane, resulting in a loss of dendritic spines.[40] An increase in SUMO2 activity conferred by SBT02 could potentially dysregulate this process and thereby lead to the observed reduction in Aβ toxicity.

mGluR5 has an impact on these LTP-related processes through its ability to regulate AMPAR endocytosis.[47] Activation of mGluR5 has also been found to cause the retention of the Ubc9 E2 ligase within dendritic spines.[10] This results in the regulation of SUMO modification of proteins with synapse and modulation of synaptic plasticity. It has also been shown that allosteric modulators of mGluR5 can alter amyloid pathology and toxicity in different manners. Negative modulators, for example, reverse cognitive impairments in APP transgenic by reducing amyloid pathology.[48] Conversely, positive modulators are also able to restore cognitive function and reverse LTP impairments and synaptic loss, similar to SBT02, but have no effect on amyloid pathology.[49,50] Given the similar activities of mGluR5 modulators and SBT02, it is possible that they have overlapping mechanisms of action. Additional investigations into SBT02 and its activity within synaptic compartments are required to substantiate its underlying mechanisms of action to determine if this is indeed the case.

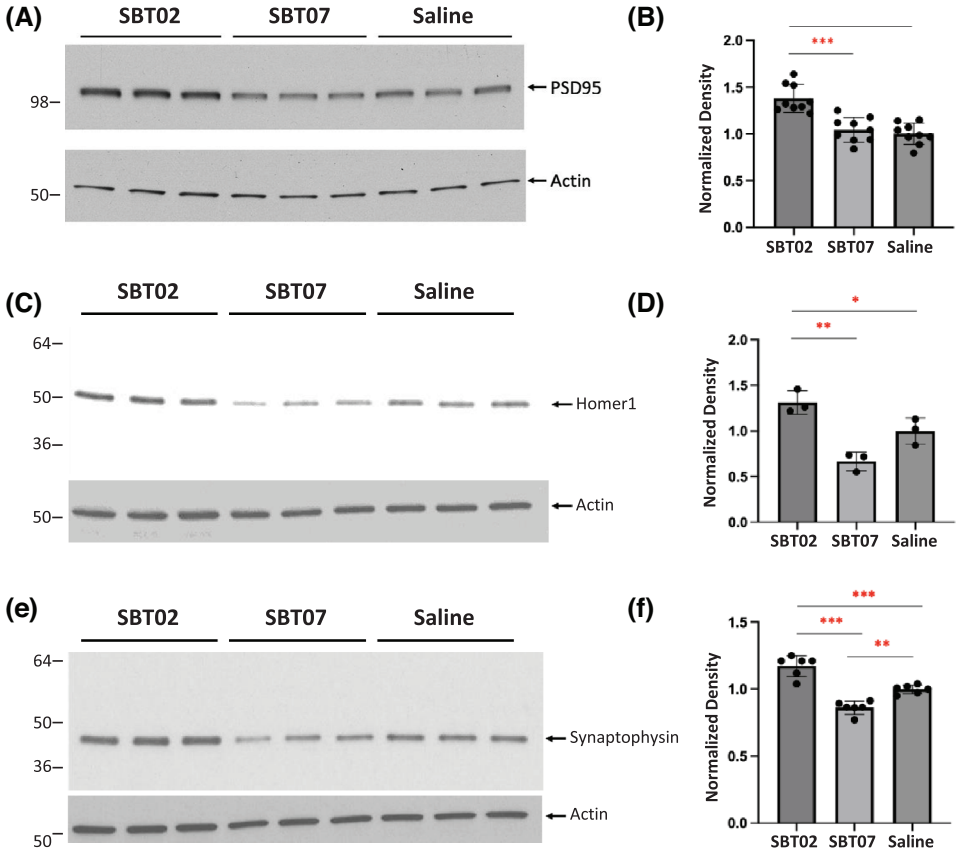

FIGURE 8 Synaptic markers in STB02-treated APP transgenic mice. (A) Immunoblot for the post-synaptic PSD-95 from brain homogenates (cortex-hippocampus combined) indicates an increase in SBT02-treated mice as compared to mice treatment with SBT07 or saline. (B) Quantification of PSD-95 immunoreactivity and the increased levels in SBT02-treated mice. (C) Immunoblot for the presynaptic Homer1 from brain homogenates (cortex-hippocampus combined) indicating an increase in SBT02-treated mice as compared to mice treatment with SBT07 or saline. (D) Quantification of Homer1 immunoreactivity and the significantly increased levels in SBT02-treated mice. (E) Immunoblot for synaptophysin in the treated mice indicates an increase similar to that of the mice administered SBT02. (F) Quantification of the synaptophysin levels showing a statistical significance increase in the SBT02-treated animals. $^{***}p < 0.001$; $^{**}p < 0.01$; $^{*}p < 0.05$, by Tukey's multiple comparison test following ordinary one-way ANOVA. ANOVA, analysis of variance; APP, amyloid precursor protein.

Another important finding obtained through our studies is that SBT02 has high brain bioavailability and is well tolerated at therapeutic doses. This opens the possibility of using the peptide as a therapeutic against AD. Thus SBT02 represents a novel and potentially effective therapy to slow the progression of disease and, more critically, restore cognitive function in patients who have been diagnosed with later-stage AD. In addition, our initial studies revealed that some of the first targets of SUMOylation related to neurodegenerative diseases were the microtubule-associated tau protein and α-synuclein, suggesting that SUMO modifications may have wider implications in AD and possibly Parkinson's disease.[51] Subsequent studies revealed that SUMO1 modification of tau resulted in increased phosphorylation, enhanced aggregation, and reduced catabolism.[14] Based on these results, it is conceivable that SUMO2 and SBT02 treatment may have beneficial effects on the neurofibrillary tangle pathology of AD comparable to the findings of the current investigation of amyloid pathology. Our related studies, which have crossed the SUMO2 transgenics with an AD-related tau model, have demonstrated a similar prevention of cognitive deficits and LTP impairment that did not affect the underlying tau pathology.[32,52] Therefore, these data cumulatively indicate that SUMO2 has therapeutic potential for multiple targets in neurodegenerative diseases and may be more broadly applicable.

Future investigations need to be conducted to determine the precise targets of SBT02 by the identification of proteins that are conjugated in the APP transgenics. This will point to the underlying mechanism of action and possibly refinement of the potency and specificity of SUMO2 biologics for the treatment of AD and potentially other neurodegenerative diseases. We believe these findings open a new avenue for AD therapeutics, which may be particularly effective either alone or in conjunction with other approaches targeting Aβ, such as immunotherapies. Such combinations would provide enhanced synaptic function with an effective amyloid clearance strategy.

ACKNOWLEDGMENTS

The authors thank Luca Colnaghi for cloning of a *SUMO2* version in a bacterial plasmid expression vector, which was later modified, and for helpful discussions during the early stages of the project. They also thank the technical contributions by Ms. Kathy Ha, Ms. Ling Wu,

and Sara Palacino for technical support. This work was supported by the Canadian Institutes of Health Research (PJT-173497 to P.E.F.), the Weston Brain Institute (TR192065 to P.E.F.), the Alzheimer's Association (AARG 17-505136 to L.F.), National Institutes of Health (NIH-NINDS R01NS110024 and R01NS049442 to O.A., NIH R01NS134902 to L.F.), the Japanese Society for the Promotion of Science (JSPS) for a Fund for the Promotion of Joint International Research (Fostering Joint International Research) (17KK0197 to S.M.), and Grant-in-Aid for Scientific Research (C) (21K06759 to S.M.).

CONFLICT OF INTEREST STATEMENT

L.F., O.A., and P.E.F. are co-inventors on a patent application for the use of SUMO2 mimetic peptides in Alzheimer's disease. N.W., E.K.A., S.M., H.T., K.S., K.H., H.Y., A.S., E.A., F.O., A.M., and T.K. have nothing to disclose. Author disclosures are available in the Supporting Information.

CONSENT STATEMENT

Consent was not necessary, since no human subjects were included in this study.

REFERENCES

1. Karran E, De Strooper B. The amyloid hypothesis in Alzheimer disease: new insights from new therapeutics. *Nat Rev Drug Discovery*. 2022;21(4):306-318. doi:10.1038/s41573-022-00391-w
2. Tzioras M, McGeachan RI, Durrant CS, Spires-Jones TL. Synaptic degeneration in Alzheimer disease. *Nat Rev Neurol*. 2023;19(1):19-38. doi:10.1038/s41582-022-00749-z
3. Henley JM, Seager R, Nakamura Y, Talandyte K, Nair J, Wilkinson KA. SUMOylation of synaptic and synapse-associated proteins: an update. *J Neurochem*. 2021;156(2):145-161. doi:10.1111/jnc.15103
4. Chang HM, Yeh ETH. Sumo: from bench to bedside. *Physiol Rev*. 2020;100(4):1599-1619. doi:10.1152/physrev.00025.2019
5. Gong L, Yeh ETH. Characterization of a family of nucleolar SUMO-specific proteases with preference for SUMO-2 or SUMO-3. *J Biol Chem*. 2006;281(23):15869-15877. doi:10.1074/jbc.M511658200
6. Schorova L, Martin S. Sumoylation in synaptic function and dysfunction. *Front Synaptic Neurosci*. 2016;8(APR):9. doi:10.3389/fnsyn.2016.00009
7. Colnaghi L, Russo L, Natale C, et al. Super resolution microscopy of SUMO proteins in neurons. *Front Cell Neurosci*. 2019;13:486. doi:10.3389/fncel.2019.00486
8. Girach F, Craig T, Rocca D, Henley J. RIM1α SUMOylation is required for fast synaptic vesicle exocytosis. *Cell Rep*. 2013;5(5):1294-1301. doi:10.1016/j.celrep.2013.10.039
9. Craig TJ, Anderson D, Evans AJ, Girach F, Henley JM. SUMOylation of Syntaxin1A regulates presynaptic endocytosis. *Sci Rep*. 2015;5:17669. doi:10.1038/srep17669
10. Loriol C, Cassé F, Khayachi A, et al. mGlu5 receptors regulate synaptic sumoylation via a transient PKC-dependent diffusional trapping of Ubc9 into spines. *Nat Commun*. 2014;5:5113. doi:10.1038/ncomms6113
11. Khayachi A, Gwizdek C, Poupon G, et al. Sumoylation regulates FMRP-mediated dendritic spine elimination and maturation. *Nat Commun*. 2018;9(1):757. doi:10.1038/s41467-018-03222-y
12. Drisaldi B, Colnaghi L, Fioriti L, et al. SUMOylation is an inhibitory constraint that regulates the prion-like aggregation and activity of CPEB3. *Cell Rep*. 2015;11(11):1694-1702. doi:10.1016/j.celrep.2015.04.061
13. Fioriti L, Myers C, Huang YY, et al. The persistence of hippocampal-based memory requires protein synthesis mediated by the prion-like protein CPEB3. *Neuron*. 2015;86(6):1433-1448. doi:10.1016/j.neuron.2015.05.021
14. Luo H-B, Xia Y-Y, Shu X-J, et al. SUMOylation at K340 inhibits tau degradation through deregulating its phosphorylation and ubiquitination. *Proc Nat Acad Sci USA*. 2014;111(46):16586-16591. doi:10.1073/pnas.1417548111
15. Rott R, Szargel R, Shani V, et al. SUMOylation and ubiquitination reciprocally regulate α-synuclein degradation and pathological aggregation. *Proc Nat Acad Sci USA*. 2017;114(50):13176-13181. doi:10.1073/pnas.1704351114
16. Saitoh H, Hinchey J. Functional heterogeneity of small ubiquitin-related protein modifiers SUMO-1 versus SUMO-2/3. *J Biol Chem*. 2000;275(9):6252-6258.
17. Ford L, Fioriti L, Kandel ER. Ubiquitination and SUMOylation of amyloid and amyloid-like proteins in health and disease. Article. *Curr Issues Mol Biol*. 2020;35:195-230. doi:10.21775/cimb.035.195
18. Marmor-Kollet H, Siany A, Kedersha N, et al. Spatiotemporal proteomic analysis of stress granule disassembly using APEX reveals regulation by SUMOylation and links to ALS pathogenesis. *Mol Cell*. 2020;80(5):876-891.e6. doi:10.1016/j.molcel.2020.10.032
19. Ford L, Asok A, Tripp AD, et al. CPEB3 low-complexity motif regulates local protein synthesis via protein-protein interactions in neuronal ribonucleoprotein granules. *Proc Nat Acad Sci USA*. 2023;120(6):e2114747120. doi:10.1073/pnas.2114747120
20. Knock E, Matsuzaki S, Takamura H, et al. SUMO1 impact on Alzheimer disease pathology in an amyloid-depositing mouse model. *Neurobiol Dis*. 2018;110:154-165. doi:10.1016/j.nbd.2017.11.015
21. Matsuzaki S, Lee L, Knock E, et al. SUMO1 affects synaptic function, spine density and memory. *Sci Rep*. 2015;5:10730-10730. doi:10.1038/srep10730
22. Lee L, Dale E, Staniszewski A, et al. Regulation of synaptic plasticity and cognition by SUMO in normal physiology and Alzheimer's disease. *Sci Rep*. 2014;4:7190-7190. doi:10.1038/srep07190
23. Wang Z, Wang R, Sheng H, Sheng SP, Paschen W, Yang W. Transient ischemia induces massive nuclear accumulation of SUMO2/3-conjugated proteins in spinal cord neurons. *Spinal Cord*. 2013;51(2):139-143. doi:10.1038/sc.2012.100
24. Chishti MA, Yang DS, Janus C, et al. Early-onset amyloid deposition and cognitive deficits in transgenic mice expressing a double mutant form of amyloid precursor protein 695. *J Biol Chem*. 2001;276(24):21562-21570. doi:10.1074/jbc.M100710200
25. Jiang Y, Mullaney KA, Peterhoff CM, et al. Alzheimer's-related endosome dysfunction in down syndrome is Aβ-independent but requires APP and is reversed by BACE-1 inhibition. *Proc Nat Acad Sci USA*. 2010;107(4):1630-1635. doi:10.1073/pnas.0908953107
26. Degasperi A, Birtwistle MR, Volinsky N, Rauch J, Kolch W, Kholodenko BN. Evaluating strategies to normalise biological replicates of western blot data. *PLoS ONE*. 2014;9(1):e87293. https://doi.org/10.1371/journal.pone.0087293
27. Satoh K, Abe-Dohmae S, Yokoyama S, St. George-Hyslop P, Fraser PE. ATP-binding cassette transporter A7 (ABCA7) loss of function alters Alzheimer amyloid processing. *J Biol Chem*. 2015;290(40):24152-24165. doi:10.1074/jbc.M115.655076
28. Von Mollard GF, Südhof TC, Jahn R. A small GTP-binding protein dissociates from synaptic vesicles during exocytosis. *Nature*. 1991;349(6304):79-81. doi:10.1038/349079a0
29. Abizaid A, Liu Z-W, Andrews ZB, et al. Ghrelin modulates the activity and synaptic input organization of midbrain dopamine neurons while promoting appetite. *J Clin Invest*. 2006;116(12):3229-3239. doi:10.1172/JCI29867
30. Dohgu S, Nishioku T, Sumi N, et al. Adverse effect of cyclosporin A on barrier functions of cerebral microvascular endothelial cells after hypoxia-reoxygenation damage in vitro. *Cell Mol Neurobiol*. 2007;27(7):889-899. doi:10.1007/s10571-007-9209-2

31. Puzzo D, Argyrousi EK, Staniszewski A, et al. Tau is not necessary for amyloid-ß-induced synaptic and memory impairments. *J Clin Invest*. 2020;130(9):4831-4844. doi:10.1172/JCI137040
32. Orsini F, Argyrousi E, Restelli E, et al. SUMO2 protects against tau-induced synaptic and cognitive dysfunction. *Biorxiv*. 2022. 2022.11.11.516192. doi:10.1101/2022.11.11.516192
33. Datwyler AL, Lättig-Tünnemann G, Yang W, et al. SUMO2/3 conjugation is an endogenous neuroprotective mechanism. *J Cereb Blood Flow Metab*. 2011;31(11):2152-2159. doi:10.1038/jcbfm.2011.112
34. Binda CS, Heimann MJ, Duda JK, Muller M, Henley JM, Wilkinson KA. Analysis of protein sumoylation and SUMO pathway enzyme levels in Alzheimer's disease and down's syndrome. *Opera Medica et Physiologica*. 2017;3(1):19-24. doi:10.20388/omp2017.001.0042
35. Hendriks IA, Lyon D, Su D, et al. Site-specific characterization of endogenous SUMOylation across species and organs. *Nat Commun*. 2018;9(1):2456. doi:10.1038/s41467-018-04957-4
36. Lamoliatte F, Caron D, Durette C, et al. Large-scale analysis of lysine SUMOylation by SUMO remnant immunoaffinity profiling. *Nat Commun*. 2014;5:5409. doi:10.1038/ncomms6409
37. Pronot M, Kieffer F, Gay AS, et al. Proteomic identification of an endogenous synaptic SUMOylome in the developing rat brain. *Front Mol Neurosci*. 2021;14:780535. doi:10.3389/fnmol.2021.780535
38. Pronot M, Poupon G, Pizzamiglio L, et al. Bidirectional regulation of synaptic SUMOylation by Group 1 metabotropic glutamate receptors. *Cell Mol Life Sci*. 2022;79(7):378. doi:10.1007/s00018-022-04405-z
39. Craig TJ, Jaafari N, Petrovic MM, Rubin PP, Mellor JR, Henley JM. Homeostatic synaptic scaling is regulated by protein SUMOylation. *J Biol Chem*. 2012;287(27):22781-22788. doi:10.1074/jbc.M112.356337
40. Hsieh H, Boehm J, Sato C, et al. AMPAR removal underlies Aβ-induced synaptic depression and dendritic spine loss. *Neuron*. 2006;52(5):831-843. doi:10.1016/j.neuron.2006.10.035
41. Lüscher C, Huber KM. Group 1 mGluR-dependent synaptic long-term depression: mechanisms and implications for circuitry and disease. *Neuron*. 2010;65(4):445-459. doi:10.1016/j.neuron.2010.01.016
42. Um J, Kaufman A, Kostylev M, et al. Metabotropic glutamate receptor 5 is a coreceptor for Alzheimer Aβ oligomer bound to cellular prion protein. *Neuron*. 2013;79(5):887-902. doi:10.1016/j.neuron.2013.06.036
43. Renner M, Lacor PN, Velasco PT, et al. Deleterious effects of amyloid β oligomers acting as an extracellular scaffold for mGluR5. *Neuron*. 2010;66(5):739-754. doi:10.1016/j.neuron.2010.04.029
44. Steele JW, Brautigam H, Short JA, et al. Early fear memory defects are associated with altered synaptic plasticity and molecular architecture in the TgCRND8 Alzheimer's disease mouse model. *J Comp Neurol*. 2014;522(10):2319-2335. doi:10.1002/cne.23536
45. Adalbert R, Nogradi A, Babetto E, et al. Severely dystrophic axons at amyloid plaques remain continuous and connected to viable cell bodies. *Brain*. 2009;132(2):402-416. doi:10.1093/brain/awn312
46. Jaafari N, Konopacki FA, Owen TF, et al. SUMOylation is required for glycine-induced increases in AMPA receptor surface expression (ChemLTP) in hippocampal neurons. *PLoS ONE*. 2013;8(1):e52345. doi:10.1371/journal.pone.0052345
47. Nakamoto M, Nalavadi V, Epstein MP, Narayanan U, Bassell GJ, Warren ST. Fragile X mental retardation protein deficiency leads to excessive mGluR5-dependent internalization of AMPA receptors. *Proc Nat Acad Sci USA*. 2007;104(39):15537-15542. doi:10.1073/pnas.0707484104
48. Hamilton A, Vasefi M, Vander Tuin C, McQuaid RJ, Anisman H, Ferguson SSG. Chronic pharmacological mGluR5 inhibition prevents cognitive impairment and reduces pathogenesis in an Alzheimer disease mouse model. *Cell Rep*. 2016;15(9):1859-1865. doi:10.1016/j.celrep.2016.04.077
49. Haas LT, Salazar SV, Smith LM, et al. Silent allosteric modulation of mGluR5 maintains glutamate signaling while rescuing Alzheimer's mouse phenotypes. *Cell Rep*. 2017;20(1):76-88. doi:10.1016/j.celrep.2017.06.023
50. Spurrier J, Nicholson L, Fang XT, et al. Reversal of synapse loss in Alzheimer mouse models by targeting mGluR5 to prevent synaptic tagging by C1Q. *Sci Transl Med*. 2022;14(647):eabi8593. doi:10.1126/scitranslmed.abi8593
51. Dorval V, Fraser PE. Small ubiquitin-like modifier (SUMO) modification of natively unfolded proteins tau and alpha-synuclein. *J Biol Chem*. 2006;281(15):9919-9924. doi:10.1074/jbc.M510127200
52. Orsini F, Pascente R, Martucci A, et al. SUMO2 rescues neuronal and glial cells from the toxicity of P301L tau mutant. *Front Cell Neurosci*. 2024;18:1437995.

SUPPORTING INFORMATION

Additional supporting information can be found online in the Supporting Information section at the end of this article.

How to cite this article: Fioriti L, Wijesekara N, Argyrousi EK, et al. Genetic and pharmacologic enhancement of SUMO2 conjugation prevents and reverses cognitive impairment and synaptotoxicity in a preclinical model of Alzheimer's disease. *Alzheimer's Dement*. 2025;21:e70030. https://doi.org/10.1002/alz.70030